C.3

SANDIA REPORT

SAND96–1948 • UC–401
Unlimited Release
Printed August 1996

Unified Model of the rf Plasma Sheath Part II – Asymptotic Connection Formulae

Merle E. Riley

Prepared by
Sandia National Laboratories
Albuquerque, New Mexico 87185 and Livermore, California 94550
for the United States Department of Energy
under Contract DE-AC04-94AL85000

Approved for public release; distribution is unlimited.

SF2900Q(8-81)

Issued by Sandia National Laboratories, operated for the United States Department of Energy by Sandia Corporation.

NOTICE: This report was prepared as an account of work sponsored by an agency of the United States Government. Neither the United States Government nor any agency thereof, nor any of their employees, nor any of their contractors, subcontractors, or their employees, makes any warranty, express or implied, or assumes any legal liability or responsibility for the accuracy, completeness, or usefulness of any information, apparatus, product, or process disclosed, or represents that its use would not infringe privately owned rights. Reference herein to any specific commercial product, process, or service by trade name, trademark, manufacturer, or otherwise, does not necessarily constitute or imply its endorsement, recommendation, or favoring by the United States Government, any agency thereof or any of their contractors or subcontractors. The views and opinions expressed herein do not necessarily state or reflect those of the United States Government, any agency thereof or any of their contractors.

Printed in the United States of America. This report has been reproduced directly from the best available copy.

Available to DOE and DOE contractors from
Office of Scientific and Technical Information
PO Box 62
Oak Ridge, TN 37831

Prices available from (615) 576-8401, FTS 626-8401

Available to the public from
National Technical Information Service
US Department of Commerce
5285 Port Royal Rd
Springfield, VA 22161

NTIS price codes
Printed copy: A04
Microfiche copy: A01

SAND96-1948
Unlimited Release
Printed August, 1996

Distribution
Category UC-401

Unified Model of the rf Plasma Sheath
Part II - Asymptotic Connection Formulae

Merle E. Riley
Laser, Optics, and Remote Sensing Department 1128
Sandia National Laboratories
Albuquerque, NM 87185-1423

Abstract

A previously-developed approximation to the first integral of the Poisson equation enables one to obtain solutions for the voltage-current characteristics of a radio-frequency (rf) plasma sheath that are valid over the whole range of inertial response of the ions to an imposed rf voltage or current-specified conditions. The theory reproduced the time-dependent voltage-current characteristics of the two extreme cases corresponding to the Lieberman rf sheath theory and the Metze-Ernie-Oskam theory. In this paper the sheath model is connected to the plasma bulk description, and a prescription is given for the ion relaxation time constant, which determines the time-dependent ion impact energy on the electrode surface. It appears that this connected model should be applicable to those high density, low pressure plasmas in which the Debye length is a small fraction of the ion mean free path, which itself is a small fraction of the plasma dimension.

Contents

1. Introduction 4

2. Basic Foundations of the Plasma Model 6

3. The Four Regions of the Plasma 11
   - 3.1 The Ambipolar Diffusion Region I of the Bulk Plasma 11
   - 3.2 Neutral Region II and the Pre-sheath Region IIA 12
   - 3.3 The Transition Region III 14
   - 3.4 The Child-Langmuir Region IV 15

4.0 the Connection Algorithms 17
   - 4.1 Connection of I and II 17
   - 4.2 Connection of II and III 17
   - 4.3 Discussion of the Connected Solutions 22
     - 4.3.1 Summary of Regional Decomposition 22
     - 4.3.2 Boundary Conditions for Ambipolar Region I 23
     - 4.3.3 The Fully Connected QSS Result 24

5. Time-Dependent Ion Motion in the Sheath 27

6. Circuit Description Including Sheath Model, Examples 31
   - 6.1 Case of an Isolated Sheath with Applied rf bias 33
   - 6.2 Testing of Sheath Model where E_0 is Zero 34
   - 6.3 Testing of Sheath Model with Nonzero E_0 35

7. Conclusion 36

Acknowledgment

The support of The US Department of Energy of this work under contract DE-AC04-94AL85000 with Sandia National Laboratories is gratefully acknowledged.

1. Introduction

Sheath models have generally concerned themselves with the sheath as an isolated collisionless phenomenon near the material wall bounding a plasma.[1-3] In this report I will make an analysis that attempts to remove this restriction. Although the arguments are somewhat circuitous, I will develop a model that should be applicable to low pressure, high density plasmas which are driven by inductive coupling. The analysis does not apply to plasmas in which the sheath motion is on the order of the plasma size (capacitively coupled systems).

Lieberman's[1] theory of an rf-driven plasma sheath leads to an analytic solution for the anharmonic voltage required to produce a prescribed sinusoidal rf displacement current in the electrons. The model assumes that the electrons are cold in the sense that the electron density distribution is equal to the ion density inside the sharp electron boundary, and is zero towards the wall or electrode. There is no dc current except for the ion flow to the wall, and all the rf current is due to the oscillation of the electron boundary within the sheath, which is a displacement current. The time-independent ion density distribution within the sheath is computed self-consistently assuming that the ions see only the time average of the potential. In other words, the ions are completely inertial, responding only to the average field. The limitations of this model are mainly due to a lack of electron particle current to the wall.

Another model for an rf plasma sheath is that of Metze, Ernie, and Oskam,[2] which assumes that the electrons and the ions both respond instantaneously to an imposed time variation of the sheath potential. This is a quasi-steady state (QSS) model of the particle dynamics in which the ions as well as the electrons are effectively inertialess because they respond to a slowly varying field. This model includes electron particle current to the wall, as well as ion current and electron displacement currents. This model becomes accurate as the applied fields approach the dc limit.

It is obvious that a model that connects these two limiting theories would be of importance in the simulation of plasma sheath dynamics. Such a model has been developed[3] and appears to be fairly robust. As a computational model formulated as an ordinary differential equation in time connecting the overall sheath potential and total plasma current, it is capable of incorporating boundary conditions expressed as either time-dependent potential or current. The model is a generalization of the QSS model, with a controlled amount of inertial response of

the ions added into the theory by means of an approximate first integral of the Poisson equation and a time damping procedure for simulation of the average ion response.

In this report I review the sheath model[3] and show how to obtain a fully connected plasma-to-sheath transition based on asymptotic analysis. Divergences are eliminated or irrelevant and the physics is well defined throughout. In Section 2, I present the basic global description of the whole plasma. Section 3 discusses various regions of the plasma as isolated approximations to the general plasma equations, Section 4 presents the connection formulae between the regions, and Section 5 develops the approximation for the ion motion in an rf-driven sheath. In Section 6 I present an argument for the ion relaxation time constant that is used in the time-dependent differential equation for the ion energy in the sheath.

2. Basic Foundations of the Plasma Model

Some aspects of plasmas require a kinetic description -- details of the particle energy distribution and subtleties in heating mechanisms come to mind. However, properties such as current-voltage relations and densities are generally obtainable with good accuracy from a fluid description. In this section I present the fluid equations of motion (EOM) which are generally applicable to the low-pressure, high-density plasmas of interest.[4-7] References 6 and 7 are particularly valuable for a discussion of the general sheath problem.

Consider a one-dimensional, time-dependent plasma in contact with material walls or electrodes. The one-dimensional nature is not so much a restriction as a condition that the plasma is being analyzed in the vicinity of the walls. The coordinate is just the local outward-directed normal to the wall. The major charged particles in the plasma are a positive ion species and electrons, of number densities n_i and n_e. The plasma ions are described by the continuity equation,

$$\dot{n}_i + (n_i u_i)' = r_i \,, \tag{1}$$

where u_i is the ion fluid velocity, and r_i is the volume ionization source rate, and by the momentum equation,

$$\dot{u}_i + u_i u_i' = \frac{e}{m_i} E - \nu_i u_i \,, \tag{2}$$

where $E = -\phi'$ is the electric field, ν_i is the sum of momentum transfer and ionization collision frequencies, and the ion diffusion term has been neglected. Ion thermal diffusion is dominated by ambipolar diffusion in the bulk, and it is unimportant in the sheath transition region. The ions are generally cold compared to the electrons. There is a constant background neutral density N_o, which is typically considerably larger than the plasma density. The collision frequency is related to background density, ion velocity, and an ion-neutral scattering cross section:

$$\nu_i = N_o \, \mathrm{v}_i \, \sigma_i \,. \tag{3}$$

The velocity v_i in this relation is approximately the larger of the magnitude of the ion fluid velocity or the ion thermal velocity. In and near the sheath region it will be the ion fluid velocity.

The electrons are assumed to be in an equilibrium distribution at temperature T_e in the plasma. This is reasonable because of the electron's mean energy (a few eV) and light mass, the high plasma density, and the low pressure, all of which contribute to the rapid establishment of thermal equilibrium among the electrons. I do not account for electron inertia which is unimportant throughout the radio-frequency range of interest, at least once the means of energy input to the plasma and ionization rate are specified. In other words the electrons obey the quasi-steady-state Boltzmann equation distribution in the potential field. This relation can be expressed in either differential form, or in integral form using values at some reference point x_o within the plasma bulk:

$$\begin{aligned} n_e' / n_e &= e\phi' / kT_e , \\ n_e &= n_o \exp(e(\phi - \phi_o) / kT_e), \end{aligned} \tag{4}$$

where ϕ is the potential. The only requirement on the reference point is that the electron and ion densities may be taken to be equal there -- thus it does not lie in the sheath. The differential form of the Boltzmann distribution in Eq.(4) may be obtained directly by equating the large electron mobility and diffusion terms in the drift-diffusion approximation to the electron fluid momentum equation (not shown). This is an argument that may be used to derive the equilibrium distribution of the electrons.

Poisson's equation describes the collective interaction of the charged species:

$$\phi'' = -\frac{e}{\varepsilon_o}(n_i - n_e) . \tag{5}$$

All other symbols are as usually defined.

The first task is to scale these equations so that all redundant information is removed. First the potential and electric field are scaled with the presumed constant electron temperature:

$$\phi|_{new} = e\,\phi|_{old} \,/\, kT_e\,,$$
$$E|_{new} = e\,E|_{old} \,/\, kT_e\,. \tag{6}$$

The Bohm (sonic) velocity is used to scale the ion velocity to u,

$$u_i = u\,u_B\,, \quad u_B = (kT_e \,/\, m_i)^{1/2}\,, \tag{7}$$

and the ion mean free path, λ_i, is used to scale the space coordinate from x to s:

$$x = s\,\lambda_i\,, \quad \lambda_i = 1 \,/\, N_o\,\sigma_i\,,$$
$$\nu_i = \mathrm{v}_i \,/\, \lambda_i\,. \tag{8}$$

The time variable t is scaled with the ratio of the ion collision length to Bohm velocity in order to complete the transformation to dimensionless variables:

$$\tau = \frac{u_B}{\lambda_i}\,t\,. \tag{9}$$

This time scaling will not be used much since the analysis of the equations will be done for the most part in the quasi-steady-state approximation where the time variable does not appear. One notes that the "unit" of time is roughly the mean time between collisions of a few-eV ion. The prime and over dot conventions will denote derivatives with respect to the scaled variables.

Introducing Eqs.(7)-(9) into the continuity Eq.(1) gives:

$$\dot{n}_i + (n_i\,u)' = \frac{\lambda_i}{u_B}\,r_i \equiv r\,, \tag{10}$$

Applying all of Eqs.(6)-(9) to the momentum Eq.(2) gives:

$$\dot{u} + u\,u' + \phi' + u\,\mathrm{v} = 0\,, \tag{11}$$

where $\mathrm{v} = \mathrm{v}_i \,/\, u_B$ is the scaled magnitude of either the ion fluid velocity or the thermal velocity. The Boltzmann Eq.(4) becomes:

$$n_e' / n_e = \phi' ,$$
$$n_e = n_o \exp(\phi - \phi_o) . \tag{12}$$

The one additional scaling to be done is to introduce the Debye length λ_o characteristic of the plasma density n_o at reference point x_o :

$$\lambda_o^2 = \varepsilon_o kT_e / e^2 n_o , \tag{13}$$

I introduce Eqs.(6), (8), and (13) into the Poisson Eq.(5) to have:

$$\varepsilon^2 \phi'' = -(n_i - n_e) / n_o ,$$
$$\varepsilon = \lambda_o / \lambda_i . \tag{14}$$

For the low-pressure, high-density plasmas that we are investigating, ε is a small number because the Debye length is much smaller than the ion collision length. ε is the most important measure of the size of the sheath compared to the bulk. Note that I have not explicitly scaled the number densities, but the Debye length contains the "reference" bulk plasma density. Eqs.(10), (11), (12), and (14) constitute the general description of the plasma.

One restriction that it will be necessary to make on the general description is the quasi-steady-state (QSS) approximation in which all $\dot{y} \approx 0$. This is an ion response approximation and is dealt with in the sheath region by means of the sheath model developed previously.[3] I invoke the QSS and collect the scaled equations, giving:

$$(n_i u)' = r ,$$
$$u u' + \phi' + u \mathrm{v} = 0 ,$$
$$n_e' / n_e = \phi' ,$$
$$\varepsilon^2 \phi'' = -(n_i - n_e) / n_o . \tag{15}$$

The equations within Eq.(15) are the basis for the analytic theory presented in this work. They are assumed to provide an adequate description (so-called exact within certain models for the electronic motion) of the plasma from the bulk to the

material wall. Basically, all developments will begin with Eq.(15) as a consistent starting point and develop approximations based on the smallness of ε. This affords a neat mathematical description of the approximations necessary to describe the transition from the bulk plasma to the wall.

The work of Godyak and Sternberg[6] is very close to the asymptotic analysis presented here. The major difference of course is the final sheath model for the ion response in an rf field.[3]

A comment should be made about the distance scaling used in this report. The use of Eq.(8) assumes that the cross section for ion velocity relaxation is constant. This may not true in general. For ion-neutral momentum transfer due to elastic scattering, the product of $\mathrm{v}\,\sigma(\mathrm{v})$ is nearly constant due to the "Maxwell molecule" effect for $1/r^4$ interactions. Thus it may be necessary to scale distance with the ion mean free path at a particular velocity or energy. If $\mathrm{v}\,\sigma(\mathrm{v})$ is constant, the functional form of the scaled momentum equation changes. In fact, if the mean free path at the Bohm velocity is chosen, the term $u\,\mathrm{v}$ in Eqs.(11) and (15) and the term u^2 in Eqs.(20) and (24), and in other places, just become u. The form of the analytic solution for the coordinate in terms of ion fluid velocity to be written down in Section 3.2, Eq.(21) changes, but this has no practical effect on the results, as it affects only the divergent character of the field in region IIA.

I will now proceed with the description of the various regions in order to derive useful new information about the sheath relation to the plasma bulk. This analysis will argue for the recognition of four distinct regions within a low pressure, high density plasma. Progressing from the bulk outward, there is the ambipolar region I where the conditions for ambipolar diffusive motion of the ions are met. Next is region IIA where the plasma is effectively neutral but the ambipolar conditions are violated. Then comes the near-wall sheath region called III where the ion velocity reaches and exceeds the Bohm velocity and neutrality no longer holds. Lastly is region IV which is essentially the Child-Langmuir region at the wall which is almost totally devoid of electrons.

3. The Four Regions of the Plasma

From a mathematical point of view, the so-called regions of the plasma are defined by the approximations to the general equations of motion that afford certain approximate solutions which describe the plasma in those regions. Fortunately these regions have been explored in the past and correspond to certain physically observable features. In this Section 3, I will cover these regions individually and not develop the connection algorithms between the spatially isolated (if that is the case) regions. Connection will be addressed in Section 4.

3.1 The Ambipolar Diffusion Region I of the Bulk Plasma

This analysis could begin in Eq.(15), which is QSS, or in the full time-dependent set of equations written down earlier. I start with the earlier set to show that this approximation does not restrict the time dependence in the plasma's approximate EOM. Set ε to zero in Eq.(14). The resulting (asymptotic) solution requires $n_e = n_i \equiv n$, *i.e.* plasma neutrality. Then Eq.(12) must hold for ions as well as electrons, and the ion momentum Eq.(11) becomes:

$$\dot{u} + uu' + n'/n + u\mathrm{v} = 0. \tag{16}$$

I now estimate the size of $|\dot{u}|$ as $|uu'|$ (or even smaller if we are near QSS), and the size of $|n'/n|$ as $|u'/u|$ from analysis of the continuity equation. What this reveals is that the n'/n and $u\mathrm{v}$ terms dominate Eq.(16) if u is much less than unity (scaled units). The term uu' is negligible compared to u'/u under this condition and this is a sufficient condition for the development of the ambipolar diffusion equation. One can now retain only these two dominant terms in Eq.(16), giving, in scaled and unscaled form:

$$nu = -n'/\mathrm{v} \quad or \quad n_i u_i = -\frac{kT_e}{m_i \nu_i} n_i' \equiv -D_a n_i', \tag{17}$$

where D_a is the ambipolar diffusion coefficient.[4] Note that we can identify ν_i in the unscaled relation whether we used the ion fluid velocity or the ion thermal velocity to determine the collision frequency. Eq.(17) is the ambipolar expression for ion flux that allows Eq.(1) to be solved as a diffusion equation. Of course I

have obtained the form of the ambipolar diffusion coefficient that has the electron temperature much higher than the ion temperature. The two primary conditions required for accuracy of this approximation are that the plasma be quasi-neutral and the ion velocity be much less than the Bohm velocity.

From the solution to Eq.(1) or (10) *via* Eq.(17), the other physical quantities are found, in scaled and unscaled form:

$$
\begin{aligned}
n_e &= n_i = n, \\
E &= -n'/n \quad or \quad E = -\frac{kT_e}{e}\, n_i'/n_i, \\
u &= E/\mathrm{v} \quad or \quad u_i = \frac{e}{m_i \nu_i} E \equiv \mu_i E, \\
\phi &= \phi_o + \ln(n/n_o) \quad or \quad \phi = \phi_o + \frac{kT_e}{e}\ln(n_i/n_o).
\end{aligned}
\tag{18}
$$

μ_i is the ion mobility.[4] Boundary conditions (b.c.) must be formulated in order to complete the analysis. This will be the topic of a later section of this work.

3.2 Neutral Region II and the Pre-sheath Region IIA

I begin the analysis with Eq.(15) and let the dimensionless parameter ε approach zero. Using the standard arguments of asymptotic analysis,[8] all physical variables are assumed to have a Taylor series development in the ε parameter. Recall that ε is the ratio of Debye length to ion collision length. This asymptotic limit leads to the zeroth-order-in-ε, quasi-neutral equivalents of Eq.(15):

$$
\begin{aligned}
(nu)' &= r, \\
uu' + n'/n + u\mathrm{v} &= 0, \\
n'/n = \phi' &= -E, \\
n_e &= n_i = n.
\end{aligned}
\tag{19}
$$

Together Eq.(19) can be solved numerically to determine all properties of the plasma in the neutral region II (and I) if conditions can be formulated at the boundaries (b.c.). It is seen that region II includes all the plasma that is quasi-neutral - everything but the sheath itself. The relationship of the above to the

ambipolar theory of Section 3.1 just involves the size of u compared to unity. Thus ambipolar theory is just a special limit of the overall quasi-neutral region. In practice it will be convenient to decompose II into the ambipolar region I and the residual of II, to be called region IIA.

Straightforward manipulations of Eq.(19) give an analytic solution for u in terms of an indefinite integral of r once we have specified the ion collision velocity v as being either the magnitude of the fluid velocity or the ion thermal velocity. However the general solution in region II is only needed in an outer volume where we may suppose that r is zero (flux is constant) and the ion fluid velocity large enough that $\mathrm{v} = |u|$ without introducing significant error. I call this region IIA. It is basically an "ion mean free path's worth" of the plasma near the wall. Thus the simplified EOM in the outer part of region II (*i.e.* IIA) may be written (considering only orientations $u \geq 0$):

$$\begin{aligned} (nu)' &= 0, \\ u'(u - 1/u) + u^2 &= 0, \\ E = u'/u &= -\phi' , \\ n_e &= n_i = n . \end{aligned} \tag{20}$$

Henceforth I will assume $u \geq 0$ in the analysis, which means that we are considering the sheath as a right-hand boundary on the plasma. The thickness of region IIA is of $O(\lambda_i)$ or $O(1)$ is scaled distance units. Without loss of generality, I can impose b.c. of $u = 1$ (Bohm velocity) at position $s = s_1$; the analytic solutions $u(s)$ and $E(s)$ to Eq.(20) can be expressed in terms of that one integration constant,

$$\begin{aligned} s &= s_1 - \ln(u) - \tfrac{1}{2}\left(1/u^2 - 1\right), \\ E &= u^2/(1-u^2). \end{aligned} \tag{21}$$

Eq.(21) is an implicit solution for $u(s)$ with b.c. imposed at the space point s_1. It may easily be shown from Eq.(20) that the solution approaches the point s_1 with infinite slope. Thus u' (and also n' and E) is divergent at the point s_1. This divergence of the electric field as one approaches the Bohm velocity from the "inside" is a well known problem in the analysis of plasma sheaths.[5-7] It is also a

sign that the asymptotic analysis of the differential equations needs correction at the point of diverence. The other quantities are determined from the solution in Eq.(21) and b.c. at s_1. Note that Eq.(21) may be used to connect the b.c. at point s_1 to those at s_o if u_o is known at the reference point. This suggests that the reference point should lie in region IIA so that assumptions leading to Eq.(20) hold true.

The ambipolar approximation derived in Section 3.1 should be contained within the quasi-neutral approximation appropriate for the whole region II, except for the time dependence. If I assume that u is less than unity, the field expression in Eq.(21) reduces to $E \approx u^2$, which is the same as $E = u\mathrm{v} \approx u^2$ from Eqs.(17) and (18), once having set $\mathrm{v} \approx u$ because the ion collision frequency is being determined by the macroscopic ion fluid velocity near the sheath.

Thus far I have obtained solutions for the plasma that have taken advantage of the smallness of ε to avoid the very stiff numerical problem associated with doing a full numerical solution of the fluid equations coupled with the Poisson equation. Both regions I and IIA are quasi-neutral, being parts of region II. However there is a problem -- the field solution found in region IIA diverges when the ion fluid velocity reaches the Bohm velocity, corresponding to about an eV of kinetic energy. This is not acceptable if one is required to evaluate the field directly, as the ions easily reach an energy of a few or several eV upon traversing the plasma sheath potential created by the electrons and their interaction with the material wall.[4,7] Thus we are missing a valid solution in the neighborhood of the wall. This solution must carry the description through the plasma sheath where the above asymptotic solution of region IIA diverges and is not acceptable.

3.3 The Transition Region III

The results of the previous Sections 3.1 and 3.2 may be summarized as follows: we obtained an approximate asymptotic solution to the plasma fluid EOM by using the ratio of the Debye length to ion collision length as a smallness parameter. The asymptotic solution broke down at the point where the ion fluid velocity reached the Bohm velocity. Thus there is a non-uniformity involved in the approximation, and this must be corrected by some other analysis. I now will

redo the limit of $\varepsilon \to 0$ by a method of analysis[8] that leads to a uniform solution in the vicinity of the sheath.

Begin with Eq.(15) but do not yet let $\varepsilon \to 0$. Recall that this limit gave a quasi-neutral solution which was singular at $u = 1, s = s_1$. The space coordinate is now "stretched"[8] by first substituting $s = s_1 + \varepsilon z$ into Eq.(15) and then letting $\varepsilon \to 0$. Again only the zeroth-order terms in a Taylor expansion in ε of the dependent variables are retained. The space derivatives now dominate the equations and the ε dependence disappears from the Poisson equation. The first two equations become complete differentials and may be integrated with two constants of integration corresponding to scaled flux and energy, Γ_1 and E_1. The result is:

$$\begin{aligned} n_i u &= \Gamma_1 , \\ \tfrac{1}{2}u^2 + \phi &= E_1 , \\ n_e' / n_e &= \phi' , \\ \phi'' &= -(n_i - n_e) / n_o . \end{aligned} \tag{22}$$

These equations can be further integrated by substituting the n_e and n_i dependence on ϕ into the Poisson equation.[2,3,5-7] This is the so-called first integral of the second order Poisson equation which relates the electric field and potential. I do not write this out because it involves three undetermined constants of integration which we cannot, at the moment, determine.

It is worth understanding the limitation of Eq.(22) due to the stretching transformation[8] which was used to derive it. The solution to Eq.(22) is only valid within a small region of size ε about the point s_1. Nevertheless this is a very important region of the plasma, as the above solution no longer requires neutrality and the equations can be interpreted as the collisionless free fall of the ions from the bulk to the material wall.[4-7] The present problem is to find how to connect the general region III solution of Eq.(22) to the solution in the neutral region II. One should note that the original coordinate scaling, as given in Eq.(8), implied no approximations to the EOM by itself. The stretching transformation though, which is the same as a coordinate scaling with the *Debye length*, has been used to generate an approximation based on the smallness of ε.

3.4 The Child-Langmuir Region IV

This is a well-discussed plasma region which I only briefly discuss from the perspective of what is being developed here. There would appear to be two CL (Child-Langmuir) forms that might be used: collisional and collisionless. The collisionless is more commonly used[4] and is obtained simply as the large-argument form of the stretched EOM presented in Eq.(22). At large argument (coordinate) the electron density vanishes exponentially and one is left with the equations:

$$\begin{aligned} n_i\, u &= \Gamma_1 \,, \\ \tfrac{1}{2}u^2 + \phi &= E_1 \,, \\ \phi'' &= -\, n_i \,/\, n_o \,. \end{aligned} \tag{23}$$

These are easy to solve if one sets Γ_1 to some known flux and E_1 to zero to fix the zero of the potential. The solution leads to useful interpretations of current and voltage relations.[4] The novel collisional CL would be obtained from Eq.(15) by scaling $\phi \to \phi / \varepsilon^2$ and $u_i \to u_i / \varepsilon$ prior to letting $\varepsilon \to 0$. This solution would *not* be limited in spatial extent. I have not developed it in any way.

The collisionless CL is of limited spatial extent because of the scaling. For this reason, region IV is really a part of region III in that the approximate solutions developed for III will be valid for the collisionless IV.

4. The Connection Algorithms

4.1 Connection of I and II

This is a very simple task. Since the ambipolar and neutral regions are both uniform in their region of overlap, one just equates the appropriate quantities at some point in the common territory. Let this point be at s_o, (scaled x_o) the so-called reference point for the potential. The region I solution requires that u be small compared to unity, and the region IIA solution requires that we be close enough to the singular point s_1 that we can neglect the ionization source in the continuity equation. Once this point is chosen, we equate ion density and flux.

4.2 Connection of II and III

This is a more complex problem, requiring the matching of solutions between stretched and unstretched regions of space. There is an analogous problem in the asymptotic (semiclassical JWKB) solution of the linear Schrodinger equation at a potential barrier. In that case the explicit solution of the stretched problem (an Airy function) can be matched to the exponential forms at a sufficient distance from the turning point. Because the Schrodinger equation is linear, it offers only conceptual guidance to the highly non-linear plasma problem.

I recapitulate some of the previous discussion. Consider the outer part, IIA, of region II together with region III. As previously argued, one may neglect the volume ionization source there as it is a small fraction of the total production (see discussion leading to Eq.(20)). If I assume that function values are known at the reference point x_o within the neutral region IIA, the general equations in Eq.(15) may be rewritten:

$$\begin{gathered} n_i u = n_o u_o , \quad n_e(x_o) = n_i(x_o) = n_o , \\ u u' + \phi' + u^2 = 0 , \\ n_e = n_o \exp(\phi - \phi_o) , \\ \varepsilon^2 \phi'' = -u_o / u + \exp(\phi - \phi_o). \end{gathered} \tag{24}$$

The independent variable does not appear in Eq.(24) explicitly. In such case the transformation,

$$\frac{d}{ds} = \frac{d\phi}{ds}\frac{d}{d\phi} = -E\frac{d}{d\phi},$$
$$\frac{d^2\phi}{ds^2} = -\frac{d}{ds}E = E\frac{dE}{d\phi}, \tag{25}$$

converts the third order differential system to a second order system of equations:

$$u\frac{du}{d\phi} + 1 = \frac{u^2}{E},$$
$$\varepsilon^2 E\frac{dE}{d\phi} = -\frac{u_o}{u} + \exp(\phi - \phi_o). \tag{26}$$

The asymptotic solution of Eq.(26) begins by assuming that all dependent variables have a Taylor or Laurent expansion in ε. The approximation of region IIA can be obtained by taking the $\varepsilon \to 0$ limit of the Taylor-expanded Eq.(26), giving the solutions at zeroth-order in ε:

$$u = u_o \exp(\phi_o - \phi), \quad E = \frac{u^2}{1-u^2}. \tag{27}$$

This is equivalent to the solution found in Section 3.2, except that here I have not yet solved for the coordinate dependence. Remember that the first equation in Eq.(27) states $n_i = n_e$. The stretched approximation of region III is obtained from Eq.(26) by first scaling the field, which is a coordinate derivative,

$$E|_{old} = \frac{1}{\varepsilon}E|_{new}, \tag{28}$$

and then letting $\varepsilon \to 0$. One obtains the zeroth-order-in-ε equations:

$$u\,du + d\phi = 0,$$
$$E\frac{dE}{d\phi} = -\frac{u_o}{u} + \exp(\phi - \phi_o). \tag{29}$$

These equations are exact differentials, and may be integrated exactly. In order to avoid any confusion, I resubstitute the ε parameter into the solution so that all quantities are the same between variables in region II and III. The general solution to Eq.(29) is

$$\begin{aligned} \tfrac{1}{2}u^2 + \phi - \phi_o &= C_1 , \\ \tfrac{1}{2}\varepsilon^2 E^2 &= u_o u + \exp(\phi - \phi_o) + C_2 . \end{aligned} \tag{30}$$

The two constants of integration must be determined by connecting Eq.(30) to the one given in Eq.(27).

The approximations for $u(\phi)$ are uniformly well behaved in both region II and III (examine Eqs.(27) and (30)); thus I can determine the constant C_1 by matching function *and* slope of the two approximate forms of $u(\phi)$. By manipulation of Eqs.(27) and (30), one can show that this requires u to be unity, which *uniquely* singles out the Bohm point, which occurs at the point called s_1 in the region II spatial solution (Eq.(21)) where E diverges. The result is:

$$\begin{aligned} \phi_1 &= \phi_o + \ln(u_o) , \\ C_1 &= \tfrac{1}{2} + \ln(u_o) . \end{aligned} \tag{31}$$

To determine C_2, note that E in Eq.(30) is the unstretched E. Matching of fields between regions IIA and III requires that this E be finite as $\varepsilon \to 0$. Determine C_2 by the $\varepsilon \to 0$ limit of Eq.(30) at constant E at the above derived match point:

$$\begin{aligned} C_2 &= \tfrac{1}{2}\varepsilon^2 E^2 - u_o u - \exp(\phi - \phi_o), \\ &\xrightarrow[\substack{\varepsilon \to 0, u \to 1 \\ \phi \to \phi_o + \ln u_o}]{} -2u_o \quad . \end{aligned} \tag{32}$$

Thus the connected form of Eq.(30) is:

$$\begin{aligned} \tfrac{1}{2}u^2 + \phi - \phi_o &= \tfrac{1}{2} + \ln(u_o), \\ \tfrac{1}{2}\varepsilon^2 E^2 &= u_o u + \exp(\phi - \phi_o) - 2u_o . \end{aligned} \tag{33}$$

Remember that this solution is valid near s_1 (in region III) and that the subscripted constants are from the reference point s_o in region II. Eq.(33) may be rewritten with the constants defined at the Bohm point instead of the point s_o. The first step in rewriting Eq.(33) is to use $n_o u_o = n_1 u_1 = n_1$ to eliminate u_o. This leaves a outside density factor at the Bohm point, n_1, which is removed by redefining the Debye length part of the ε parameter to contain reference density n_1 instead of n_o as originally defined in Eqs.(13) and (14). The result is the very neat form of the stretched equation for description about the Bohm point:

$$\begin{aligned} \tfrac{1}{2}u^2 + \phi &= \tfrac{1}{2} + \phi_1 , \\ \tfrac{1}{2}\varepsilon^2 E^2 &= u - 1 + \exp(\phi - \phi_1) - 1. \end{aligned} \tag{34}$$

The connection result may be restated to be that the zeroth-order field is zero at the Bohm point where $u = u_1$ and $n_e = n_i = n_1$. Of course u_1 is unity and it has disappeared from Eq.(34).

Numerical studies show that the velocities and densities of the approximations in regions IIA and III agree well with the precise numerical solution to Eq.(24) or (26). Remember that the *totality* of physical solutions to Eq.(26) are characterized by the value of ε and the point (u_o, ϕ_o). The very good accuracy of the velocity and density approximations is seen in the upper and lower panes of Fig.1. A series of numerical investigations not shown here demonstrate that a better connection result for the electric field than what is given in Eq.(34) can be obtained by a *constant*, but ε-dependent, phenomenological correction to E. This is the field value at the Bohm point:

$$\begin{aligned} \tfrac{1}{2}u^2 + \phi &= \tfrac{1}{2} + \phi_1 , \\ \tfrac{1}{2}\varepsilon^2 (E - E_1)^2 &= u - 1 + \exp(\phi - \phi_1) - 1 , \\ E_1 &= -\log_{10}(\varepsilon^2) . \end{aligned} \tag{35}$$

This result is what is plotted in the center pane of Fig.1. Of special note is the fact that the shift in E is *not* in the position of the constant of integration C_2 as seen in Eq.(30). Various quantities are explained in the caption. The results are very encouraging. A correction brought out by Godyak[9] is of the order of the above, although his result omits the ε-dependence contained in the log function. The

above log term can be interpreted as an improved (non-zero) value of the field *at* the Bohm point. Of course, the approximation still only agrees with the numerical solution in the proper region of phase space.

In Fig.2 I compare various treatments of the electric field. The upper pane is the best result using Eq.(35). The center pane is without the correction term, just as given in Eq.(34), and the lower pane shows the result of using the ambipolar approximation for the field in region IIA. One notes that the ambipolar approximation has the field in error by about 20% to 30% near $\phi = 0$ where it is approaching its domain of accuracy. Although it might seem that the above results are contradictory, or at best poorly defined, they are not. The correction to E is being made in the stretched region III solution where it is actually an $\sim O(1)$ addition to the $O(1/\varepsilon)$ field. In order to see this, substitute Eq.(28) into Eq.(35). Thus Eq.(34) is actually the $\varepsilon \rightarrow 0$ limit of Eq.(35), the latter being more accurate. Eq.(34) is asymptotically correct for the field as one can see that the field approaches the exact numerical solutions as one moves away from the Bohm point.

In Fig.3 I plot the quantities as a function of scaled distance to better show the comparison of the approximations to the numerical solution at and near the sheath region. Remember that the dotted quantities should agree with the solid curves on the LHS of the plots, and the dashed quantities should agree with the solid on the RHS. All in all, things are very good except for the electric field singularity of the region IIA asymptotic solution. However this nonuniformity is totally unimportant once one knows how to connect the solution to the region III approximation. The accuracy of our connection algorithm is shown by Figs.1 and 3. In Fig.4 I show the same comparison of the various field approximations as a function of space coordinate as in Fig.2 in phase space.

In the previous plots of quantities versus space coordinate, the mapping of coordinate to potential was taken from the numerical solution of the "exact" equations. It might be more informative to use the approximate mapping implied in each of the regions. In IIA we use $s(u)$ from Eq.(21) combined with $u(\phi)$ from Eq.(27) to find $s(\phi)$. This is shown in Fig.5 as the multiple-valued function of coordinate. It is obvious which branch is the correct physical one. In region III we must do the numerical integral of the field derivative as explained in the Fig.5 caption. The starting point of the numerical solution was chosen to be at the Bohm point with ϕ_1 given by Eq.(31) and s_1 by Eq.(21) in terms of $s_o = 0$ and u_o.

A numerical survey showed that adding ε to this s_1 value gave slightly better-looking results. This is what is shown in Fig.5.

4.3 Discussion of the Connected Solutions

This section will do two things: I will discuss the results and try to make reasonable sense of them, and also I will unscale the equations and write them in natural units. First of all though, let me summarize the work, grouping things by region, starting from the "outside."

4.3.1 Summary of Regional Decomposition

The wall region IV is the electron-devoid Child-Langmuir region which is a limiting form of the mathematical solution developed to cover region III. Because of this it is not necessary to discuss it separately, except to note that the spatial extent of the region is of $O(\varepsilon)$, and therefore negligible compared to the other dimensions involved with the plasma volume.

Region III extends from the material wall at $s = w$ inward to the Bohm point at $s = s_1$ and $u = 1$. In this interval, the approximate EOM are the stretched version of Eq.(15). The solution is given by Eq.(33) in first integral form. This solution is connected to the solution in the next region II by means of the constants u_o and ϕ_o. At the point $s = s_1$, the potential is given by the value in Eq.(31). The spatial extent of region III is $O(\varepsilon)$ because of the coordinate stretching: $|w - s_1| = O(\varepsilon)$. This implies that the sheath thickness is negligible compared to other dimensions.

The next region is IIA, which begins at $s = s_1$ and extends inward to $s = s_o$ where ϕ_o and u_o are specified. Within this interval, the approximate EOM is Eq.(20), whose solution is given in Eq.(21) and (27). This region is not stretched and the size is $|s_1 - s_o| = O(1)$, in scaled coordinates. The all-important solution for $u(s)$ given in Eq.(21) affords an evaluation of $u_o(s_o, s_1)$ or $s_o(u_o, s_1)$, whichever is appropriate. Note that the EOM in Eq.(24) describe both regions IIA and III.

Region II extends from $s = s_1$ inward and covers the whole bulk of the plasma. However I have decomposed II into IIA and the rest, of which the rest may be taken to consist of region I, the ambipolar region. Region I therefore extends from $s = s_o$ inward to cover the bulk plasma. The EOM are given by

Eqs.(10) and (17), for which one needs b.c. at the s_o point or surface. The approximate solution for the flux given in Eq.(17) requires neutrality and u to be restricted less than unity.

One sees that the plasma has been practically decomposed into regions I, IIA, and III. The other divisions do not seem necessary for the high-density, low pressure plasma.

4.3.2 Boundary Conditions for Ambipolar Region I

Eq.(21) allows us to specify b.c. for the ambipolar diffusion Eqs.(10) and (17). The b.c. can be imposed at a fixed distance within the material walls, on the order of an ion collision length away. The b.c. in the numerical procedure for solving the ambipolar diffusion equation necessitates n'/n, which is found from E by means of the Boltzmann distribution relation for the electrons, E in turn is found from $u_o = u(s_o)$ by means of the ion mobility, all of which is given in Eq.(18). One knows that $v=|u|$ near the sheath in these relations.

It is not practical to demand that u_o be *much* smaller than unity because the point s_o would be pushed very far into the bulk of the plasma as seen from Eq.(21). If I set $u_o = 0.5$ Eq.(21) shows $s_1 - s_o$ is 0.807 of an ion mean free path, which is typically close enough to the material boundary to avoid complications as long as the ion mean free path is a small fraction of the plasma volume, a tenet of the whole analysis. The question that immediately comes to mind is whether any significant error is introduced by just setting a b.c. of $u_o = 1$ (Bohm velocity) on the ambipolar equation for the ions. This b.c. would imply that $s_1 = s_o$ so that the boundary surface is pushed to within $O(\varepsilon)$ of the material wall. The ambipolar breaks down there in principle because of the large fluid velocity. The neutral (region II) approximation itself breaks down because of the singularities in u'. *However, no serious errors occur with the ambipolar equation with $u_o = 1$ b.c. applied at the actual material wall as long as the volume ionization sources do not vary significantly in the outer "mean-free-path's worth" of plasma volume.* This outer volume layer is assumed to be a small part of the total plasma volume. The proof that the boundary conditions cause little error is to be found in Fig.6, where I display the results of using $u=1$ b.c. on the ambipolar solution at the Bohm point at $s = s_1$. The solution to the ambipolar equation in region IIA is similar to Eq.(21):

$$s = s_1 - \tfrac{1}{2}\left(1/u^2 - 1\right),$$
$$E = u^2. \tag{36}$$

The error in velocity and density at the point $s=0$ or $u=u_o=0.5$ is about 20%. This error tends to remain fairly constant as one continues into the bulk of the plasma, *i.e.* into the region where one cannot ignore the volume source rate r of ion production as I have done here. The ignoring of r in no way compromised the above comparison of the ambipolar approximation to the quasi-neutral in region IIA.

The accuracy of Fig.6 is sufficient to convince me that the ambipolar description can be used for most high-density, low pressure plasmas with volumetric ionization sources (*i.e.* non-capacitive).

The actual physics of the sheath will be treated by the solution of the region III equations, *which have almost no feedback into the plasma bulk.* The only input is the scalar potential itself, which becomes important when several electrodes are coupled to the same plasma. Then the feedback into the plasma takes the form of current flow through the bulk. For the most part though, information flows one way through the sheath, and that is outward from the bulk. Wall b.c. have almost no effect on the state of the bulk plasma when the ionization rate is supplied inductively as opposed to capacitively.

4.3.3 The Fully Connected QSS Result

The results of this report are first written down for the quasi-steady-state limit of the plasma. In principle there is little new here as the basics have been developed previously.[2,4-7] First of all I repeat the general conditions necessary for the applicability of the basic theory, that the plasma be high density and low pressure, and driven by a volumetric ionization source. The ion-mean-free-path-to-plasma-dimension, and Debye-length-to-ion-mean-free-path ratios are assumed to be small. The plasma is described by solution of the ambipolar diffusion equations, as discussed in Section 3.1, and with b.c. as developed in Section 4.3.2. Collecting the QSS ambipolar equations, in unscaled form:

$$
\begin{aligned}
(n_i\, u_i)' &= r_i\,, \\
n_i\, u_i &= -\frac{kT_e}{m_i\, \nu_i} n_i' \equiv -D_a\, n_i'\,, \\
u_i\big|_{b.c.} &= u_B\,,
\end{aligned}
\tag{37}
$$

with the other quantities determined by the auxillary relations:

$$
\begin{aligned}
n_e &= n_i\,, \\
E &= -\frac{kT_e}{e}\, n_i' / n_i\,, \\
u_i &= \frac{e}{m_i \nu_i} E \equiv \mu_i\, E, \\
\phi &= \phi_1 + \frac{kT_e}{e} \ln(n_i / n_1).
\end{aligned}
\tag{38}
$$

Although the QSS is being emphasized here to avoid the question of time dependence, one should note that the above bulk EOM are applicable to the time dependent problem as developed in Section 3.1. In fact, the insensitivity of the bulk to the sheath b.c. tells us that the time-dependent generalization of the above equations is all that is needed for the time behaviour of the bulk plasma.

The sheath properties are found from Eq.(35). In unscaled form, Eq.(35) is:

$$
\begin{aligned}
\tfrac{1}{2} m_i\, u_i^2 + e\,\phi &= \tfrac{1}{2} kT_e + e\,\phi_1\,, \\
\tfrac{1}{2}(E - E_1)^2 &= \frac{n_1\, kT_e}{\varepsilon_o}\left(\frac{u_i}{u_B} - 1 + \exp\left(\frac{e}{kT_e}(\phi - \phi_1)\right) - 1\right), \\
E_1 &= -\frac{kT_e}{e\,\lambda_i} \log_{10}(\varepsilon^2)\,.
\end{aligned}
\tag{39}
$$

ε is the ratio of the Debye length evaluated at Bohm point to the ion mean free path, λ_i. Unfortunately not much can be done with Eq.(39) until the general circuit equations are discussed.

A simple example is the case of a zero-current condition at the wall. The electron current per area to the wall, j_e, is approximated from kinetic theory as

$$j_e = -\tfrac{1}{4} e \, \mathrm{v}_e \, n_e(x_w) \,, \tag{40}$$

where $x = x_w$ is the wall position and v_e is the thermal velocity of the electrons:

$$\mathrm{v}_e = (8kT_e \,/\, \pi m_e)^{1/2} \,. \tag{41}$$

The electron density at the wall is obtained from the Boltzmann Eq.(12) using the Bohm point as the reference. The ion current per area to the wall is just

$$j_i = e n_i(x_w) u_i(x_w) = e n_1 \, u_B \,. \tag{42}$$

The total current is set to zero which gives the sheath potential drop and the ion impact energy on the wall from Eq.(39):

$$\begin{aligned} \phi_w - \phi_1 &= -\frac{kT_e}{e} \ln\left(\frac{\mathrm{v_e}}{4u_B}\right) = -\frac{kT_e}{2e} \ln\left(\frac{m_i}{2\pi m_e}\right), \\ \tfrac{1}{2} m_i \, u_i^2 &= \tfrac{1}{2} kT_e + \tfrac{1}{2} kT_e \ln\left(\frac{m_i}{2\pi m_e}\right). \end{aligned} \tag{43}$$

Eqs.(7) and (41) were used to simplify the result. One sees that the wall potential is determined as the difference from the Bohm point in the sheath. However the ion energy is an absolute quantity. The potential distribution within the bulk can be determined from the ambipolar solution in Eq.(38) once the wall potential is fixed.

The QSS result for the potential drop in Eq.(43) is well known;[7] the new improved result in Eq.(39) is for the electric field and will be applied later.

5. Time-Dependent Ion Motion within the Sheath

The basic development thus far for a high-density, low-pressure plasma which is inductively heated to ionization is that the ambipolar diffusion model for plasma dynamics is adequate for the bulk description. Weaker bias fields that are applied to the sheath to control the ion kinetic energy, or stray fields from the induction source, do not penetrate the bulk significantly and do not affect the flux of ions from the bulk. However the ion energy must be separately determined from a sheath model[1-3] and this is reviewed here.

The basic "exact" scaled EOM for the whole plasma is the time-dependent analog of Eq.(15):

$$\begin{aligned} \dot{n}_i + (n_i u)' &= r\,, \\ \dot{u} + u u' + \phi' + u\,\mathrm{v} &= 0\,, \\ n_e / n_o &= \exp(\phi - \phi_o)\,, \\ \varepsilon^2 \phi'' &= -(n_i - n_e)/n_o\,. \end{aligned} \tag{44}$$

I have used the b.c. at some point s_o as a reference. If I proceed with the $\varepsilon \to 0$ limit directly on Eq.(44), the quasi-neutral ambipolar results of Section 3.1 can be recovered. Here we are interested in the time-dependent motion of region III; previously only the QSS was obtained in Sections 4.2.and 4.3.3. As before, we must scale or "stretch" the coordinates before obtaining an asymptotic description. The coordinate s in Eq.(44) is stretched to z and the net result of the time scaling is that it is scaled with the plasma ion frequency,[4] ω_{pi}:

$$\begin{aligned} s &\propto \varepsilon z\,, \\ \theta &= \frac{1}{\varepsilon}\tau = \frac{\lambda_i}{\lambda_o}\frac{u_B}{\lambda_i} t \\ &= \frac{u_B}{\lambda_o} t \equiv \omega_{pi}\, t\,. \end{aligned} \tag{45}$$

Remember that in Eq.(44) the time variable is already scaled as in Eq.(9). These substitutions are made and the $\varepsilon \to 0$ limit is taken, leaving at zeroth order:

$$
\begin{aligned}
\dot{n}_i + (n_i u)' &= 0 , \\
\dot{u} + u u' + \phi' &= 0 , \\
\phi'' &= -n_i / n_o + \exp(\phi - \phi_o) .
\end{aligned}
\tag{46}
$$

The reference point at s_o is independent of time. It may be argued that the Bohm point itself is independent of time to $O(\varepsilon)$. Essentially this argument begins by noting that the region IIA EOM for $\dot{u}$ predicts it to be of $O(1)$ wherever $u \approx 1$ prior to stretching. After the stretching is done the rate of change is $O(\varepsilon)$ and negligible in Eq.(46). Thus the b.c. may be converted to $n_e = n_i = n_1$, $\phi = \phi_1$, and $u = u_i / u_B = u_1 = 1$ at the Bohm point. The b.c. on the field (negative slope of potential) can either be taken to be zero or to be the first order term written down in Eq.(35) and (39).

The analysis now follows along the lines of the arguments of references 3 and 10 in order to obtain a closed-form approximation for the ion motion. Basically the time-dependent ion motion is approximated by adiabatic motion within a new potential field, $\overline{\phi}$, which must be determined. The ion density and velocity are assumed to satisfy the conservative flux and energy relations with a parametric time dependence contained in $\overline{\phi}$:

$$
\begin{aligned}
n_i u &\approx n_1 u_1 = n_1 , \\
\tfrac{1}{2} u^2 + \overline{\phi} &\approx \tfrac{1}{2} + \phi_1 .
\end{aligned}
\tag{47}
$$

Henceforth I will work with the shifted potential $\chi(x,t) = \phi(x,t) - \phi_1(t)$ and the same for $\overline{\chi}(x,t) = \overline{\phi}(x,t) - \phi_1(t)$ so as to avoid cluttering the equations with the potential and its time derivative at the Bohm point. This is the same as setting the zero of the potential at the Bohm point. I now take the reference point s_o to be at the Bohm point s_1 and combine Eqs. (46) and (47) to give the new, mildly approximated equations:

$$
\begin{aligned}
\dot{\overline{\chi}} &= -u(\overline{\chi}' - \chi') , \\
\chi'' &= -1/u + \exp(\chi) , \\
u &= \left(1 - 2\overline{\chi}\right)^{1/2} .
\end{aligned}
\tag{48}
$$

The Poisson equation in Eq.(48) cannot be integrated exactly. The first integral must be further approximated in order to obtain an explicit solution. A convenient means of arriving at this approximation is to assume that the new potential field is related to the actual field by a function of time, *i.e.*:

$$\overline{\chi} \approx \alpha(t)\chi\,. \tag{49}$$

Eq.(49) applies to the region III EOM and thus implies that the time dependent proportionality applies outside the Bohm point. Within the Bohm point, the potential is approximately invariant to the time dependence and $\phi \approx \overline{\phi}$ as argued below Eq.(46). This *ansatz* given in Eq.(49) may be shown to have motivations based on the approximations for the first integral of the Poisson equation.[3] Substitution of Eq.(49) into (48) allows the first integral to be performed on the Poisson equation, giving rise to one new constant of integration, E_0. The zeroth-order boundary conditions are $\phi = \overline{\phi} = \phi_1$ (or $\chi = \overline{\chi} = 0$) and $E = E_0$ at the $u = u_1 = 1$ point. Both ϕ_1 and E_0 can be time dependent. After the integration is performed, $\alpha(t)$ is replaced by $\overline{\chi} / \chi$ to give:

$$\begin{aligned} \dot{\overline{\chi}} &\approx -\frac{\chi'}{\chi}(1-2\overline{\chi})^{1/2}(\overline{\chi}-\chi)\,, \\ \tfrac{1}{2}(E-E_1)^2 &\approx \tfrac{1}{2}E_0{}^2 + \frac{\chi}{\overline{\chi}}\left((1-2\overline{\chi})^{1/2}-1\right) + \exp(\chi) - 1\,, \\ E_1 &= -\log_{10}(\varepsilon^2)\,. \end{aligned} \tag{50}$$

I have *ex post facto* inserted the first-order-in-ε correction to E as found in Eq.(35). This ensures that Eq.(50) reduces correctly and exactly to Eq.(35) as $\overline{\chi} \to \chi$ and $E_0 \to 0$ in the QSS limit. The first equation has the form of a damping or relaxation equation if the prefactor can be replaced by a constant. It may be argued that the constant is of order unity. It becomes, then, simply, in scaled and unscaled form:

$$\begin{aligned} \dot{\overline{\chi}} &\approx -(\overline{\chi}-\chi)\,, \\ \dot{\overline{\chi}} &\approx -\omega_{pi}(\overline{\chi}-\chi)\,. \end{aligned} \tag{51}$$

ω_{pi} has been defined in Eq.(45). Eq.(51), combined with the voltage-field first integral in Eq.(50), are the equations to be used[3,10] to determine the effective potential of the ion response in a varying potential field. The unscaled form of the first integral approximation is:

$$\tfrac{1}{2}(E-E_1)^2 = \tfrac{1}{2}E_0^2 + \frac{n_1 kT_e}{\varepsilon_o}\left(\frac{\chi}{\overline{\chi}}\left(\sqrt{1-2e\overline{\chi}/kT_e}-1\right)\right.$$
$$\left. + \exp\left(\frac{e\chi}{kT_e}\right) - 1\right), \tag{52}$$
$$E_1 = -\frac{kT_e}{e\,\lambda_i}\log_{10}(\varepsilon^2).$$

This form differs from the earlier work[3,10] in that the Mach number does not appear. Remember that potential has been shifted by the possibly time dependent value at the Bohm point.

The constant of integration E_0 is yet to be determined. The b.c. used here is that the electric field *at* the Bohm point is greater than zero (actually $E_1 + E_0(t)$), and this correction should be large enough to force the RHS of Eq.(52) to be non-negative at whatever spatial position it is evaluated. Eq.(52) reduces to Eq.(39) (unscaled Eq.(35)) in the limit of slow time variation. In this limit the constant E_0 should be identically zero. Two numerical procedures come to mind to find E_0: number one, instantaneously set $E_0(t)$ such that the RHS of Eq.(52) is non-negative as the time-dependent EOM are being solved numerically, and number two, let $E_0(t)$ "ride up" numerically to a constant value such that the RHS of Eq.(52) remains positive.[3,10] In procedure number one the time derivative of E is zero during the interval that E_0 is forced to be nonzero. In the second procedure the time derivative of E_0 can be ignored as E_0 becomes constant after a few rf cycles. The effect of these procedures will be shown later.

The work of Pointu[11] has recently come to my attention. His sheath model reduces to a linear approximation for the time-varying part of the sheath potential, and for that reason, would not seem as accurate as the other models.[1-3] His work does predict important features, however, such as the ion plasma frequency scaling of the ion sheath response.

6. Circuit Description Including Sheath Model, Examples

Two things must be obtainable from a sheath model in the context that is being pursued here. First of all, we need the current-voltage properties of the sheath so that one can write down the functional relation of the total current to the bulk plasma properties and the sheath voltage in order to include the sheath in the circuit equations for the whole system. Secondly, we need to be able to derive important kinetic properties of the sheath particles, such as the ion energies that fall through the potential drop. This will be discussed later, although it is obvious now that we are committed to using the time-dependent kinetic energy of the mono-energetic ion fluid as predicted by the damped potential, given by Eq.(47). For the moment, consider the plasma, the plasma sheaths, and external circuitry with an analysis similar to Kirchhoff's rules for writing down the circuit equations. What is needed from the sheath itself will be written down here.

The total current per area j_{tot} through the sheath is expressed as

$$\begin{aligned} j_{tot} &= j_e + j_i + j_d \,, \\ j_i &= e\, u_i\, n_i \,, \\ j_d &= \varepsilon_o \dot{E} . \end{aligned} \tag{53}$$

One can show that the above expression for the total current is constant across the sheath if the full time-dependent continuity and Poisson's equations are being solved consistently. Here we are using approximations to the dynamics, so the expression is not independent of x. The adiabatic Boltzmann approximation for the electron particle current j_e is given by Eq.(40) in terms of the electron density at the wall, which is related by a potential-drop (Boltzmann) factor in Eq.(12) to the electron density at the reference point. The continuity equation for the ions equates the ion current j_i to the value at that reference position. The electron displacement current j_d should be evaluated at the wall position to be consistent with both the point of determination of j_e and the later connection to be developed to the total sheath potential.

The displacement current is expressed as the partial time derivative of the field at the wall. Only the potential difference between the wall and the bulk plasma is a quantity accessible in the circuit equations for the system. Thus the sheath model must supply the relation of electric field to potential. In the case of a

dc sheath, or the QSS sheath model[2,3] which is based on adiabatic response of the dc model to a time-varying applied potential, one can write down the *first integral* of the Poisson equation, $E = E(\phi - \phi_1)$ and evaluate

$$\dot{E}(x,t) = \frac{dE}{d(\phi - \phi_1)}\left(\dot{\phi}(x,t) - \dot{\phi}_1(t)\right), \tag{54}$$

which completes the determination of current as a function of voltage. This can be done from the results in Section 4.3.3 immediately. Note that Eq.(54) would be simpler if written in terms of the shifted potential with respect to the Bohm point. The case of faster voltage variations in which the ions cannot track the field adiabatically requires the use of the sheath model of Section 5. The time derivative of E now necessitates the evaluation of both partial derivatives, $\partial E / \partial(\phi - \phi_1)$ and $\partial E / \partial(\overline{\phi} - \phi_1)$, in order to find $\dot{E}$ and $j_d(t)$:

$$j_d(t) = \varepsilon_o \dot{E} = \varepsilon_o \left(\frac{\partial E}{\partial \chi}\dot{\chi} + \frac{\partial E}{\partial \overline{\chi}}\dot{\overline{\chi}} \right). \tag{55}$$

These partial derivatives are found from Eq.(52), which gives $E(\chi, \overline{\chi})$ explicitly, to wit:

$$(E - E_1)\frac{\partial E}{\partial \chi} = \frac{e n_1}{\varepsilon_o}\left\{ \frac{kT_e}{e\overline{\chi}}\left(\left(1 - \frac{2e\overline{\chi}}{kT_e}\right)^{1/2} - 1 \right) + \exp\left(\frac{e\chi}{kT_e}\right) \right\}, \tag{56}$$

and

$$(E - E_1)\frac{\partial E}{\partial \overline{\chi}} = \frac{n_1 kT_e}{\varepsilon_o}\frac{\chi}{\overline{\chi}^2}\left\{ 1 - \left(1 - \frac{2e\overline{\chi}}{kT_e}\right)^{1/2} - \frac{e\overline{\chi}}{kT_e}\left(1 - \frac{2e\overline{\chi}}{kT_e}\right)^{-1/2} \right\}. \tag{57}$$

Note that I have assumed that E_0 is independent of time and potential in evaluating these partials. In practice the derivatives will be evaluated at the wall position.

6.1 Case of an Isolated Sheath with Applied rf Bias

In this section I give the numerical solution of the sheath model for an isolated sheath. A full description of the plasma would require a model of the pumping of the plasma by an inductive antenna and the ambipolar (possibly) EOM and kinetics of the plasma bulk. This is too elaborate for the purpose of illustrating the practicality and utility of the present sheath model. Thus I make some assumptions and solve the sheath as an isolated system. Previously[3,10] I showed that the present sheath model agreed with the two extreme limits of ion response, namely the highly inertial ion model of Lieberman[1] and the QSS model of Metze, Ernie, and Oskam.[2] I will use an Ar plasma with specified conditions at the Bohm point:

$$\begin{aligned} \nu_{rf} &= 13.56\,MHz\,, \\ kT_e / e &= 4\,eV\,, \\ m_i &= 40\,amu\,(\mathrm{Ar}^+), \\ n_1 &= 1.0\times 10^{17} / m^3\,, \\ N_o &= 3.535\times 10^{20} / m^3 \quad (10\,mTorr)\,, \\ \sigma_i &= 1.0\times 10^{-18}\,m^2\,(100\,\mathring{A}^2)\,. \end{aligned} \tag{58}$$

Some derived quantities are found from the above using the notation and theory developed in the text:

$$\begin{aligned} u_B &= 3.106\ km / s\,, \\ E_1 &= 5.032\ V / mm\,, \\ \lambda_i &= 2.829\ mm\,, \\ \lambda_o &= 0.0470\ mm\,, \\ \omega_{ip} &= 6.607\times 10^7 / s\,, \\ j_i &= 49.77\ A / m^2\,. \end{aligned} \tag{59}$$

The total current through the sheath is given by Eq.(53), with all quantities evaluated at the wall position. The displacement current is given by Eqs.(55)

through (57) in terms of the potential and damped (or effective ion) potential at the wall. The effective potential for the ions is found from the numerical solution of Eq.(51) at the wall. Putting this all together leaves a coupled set of ordinary differential equations in time with the wall values of the quantities as dependent variables.

The isolated plasma sheath problem can be solved numerically with either a specified applied rf voltage or run under "current control" to find the voltage that produces a specified current through the sheath.[3,10] It matters not to the numerical algorithm presented here which method is chosen, but since a capacitively-coupled rf bias with zero average current is a common arrangement, I adopt current control as the method of choice. The components of the total current per area through the sheath are:

$$j_{tot}(t) = j_{ac}\sin(2\pi\, \nu_{rf}\, t) + j_{dc}\ , \qquad j_{dc} = 0\ . \tag{60}$$

For a specified j_{ac} the equations are integrated for 800 rf cycles (intentional overkill) with a numerical step of one thousandth of an rf cycle. The last two cycles are saved for plotting of the current, voltage, and field at the wall. One should remember that the use of current control for the isolated sheath problem requires solving "backwards" for the time derivative of ϕ in terms of the current. That is to say, from Eqs.(53) and (55):

$$\frac{d\chi}{dt} = \left(\frac{\partial E}{\partial \chi}\right)^{-1}\left((j_{tot} - j_i - j_e)/\varepsilon_o - \frac{\partial E}{\partial \bar{\chi}}\dot{\bar{\chi}}\right), \tag{61}$$

All the derivatives in Eq.(61) are to be evaluated at the wall position. If the potential at the Bohm point is fixed, χ may be simply replaced by ϕ. This allows the EOM to written as a set of coupled ordinary differential equations for the wall values of the potentials and currents.

6.2 Testing of Sheath Model where E_0 is Zero

For a considerable range of rf current through the sheath with the conditions as given in Eqs.(58)-(60), roughly for $0 \le j_{ac} < 170\, A/m^2$, the integration constant E_0 can be left as zero. In Figs.7 and 8 I show typical results

for $j_{ac} = 60\,A/m^2$ and $160\,A/m^2$. The latter value of the AC current amplitude is close to the conditions where we need to make E_0 nonzero. In Figs. 9 and 10 I show the QSS prediction (the Metze, Ernie, Oskam model) for the same conditions. The QSS is seen to underestimate the potential by a good factor of two at the wall in the higher current case, and to rather poorly represent the ion energy at the wall in both cases. Remember that the damped ion potential is the ion energy at wall impact.

6.3 Testing of Sheath Model with Nonzero E_0

At and above $j_{ac} \approx 170\,A/m^2$ for the problem at hand, E_0 must be greater than zero so that the solution for E in Eq.(52) is real. This is a consequence of the nature of the approximate solution of the time-dependent sheath problem. Hopefully the size of E_0 can remain small compared to the wall values of E. In the discussion following Eq.(52), I outlined two algorithms for selecting E_0. Both of these will be tested now.

The first procedure utilized a minimum "floating" value for $E_0(t)$ such that the square root in Eq.(52) is well defined. The results are shown in Fig. 11. To be noted is the "pinning" of $E(t)$ at the minimum value of $E_1 \approx 5kV/m$ during the peak positive voltage part of the rf cycle. The second procedure, namely finding a constant value of E_0 such that the root for $E(t)$ in Eq.(52) remains real, requires us to save the maximum transient value of $E_0(t)$ as found during the time dependent integration. In practice, each time the argument of the square root was less than zero, I increased E_0^2 by $0.1(V/m)^2$ and retained the incremented value for the rest of the integration (or until a further increase was necessary). Changing the size of the increment did not affect the results significantly. These results are shown in Fig. 12. One must compare Figs. 11 and 12 carefully to find the differences. I feel that the differences are insignificant, and that the method of choosing E_0 is not so important.

7. Conclusion

First of all I should repeat what is new within this work. The empirical asymptotic connection formula presented in Eqs.(35) and (39) (scaled and unscaled) is new. This furnishes an accurate evaluation of the electric field within the sheath region for the QSS condition. The overall analysis of the connection of the regions of the plasma is novel from the point of view of the mathematics (which might be improved I suspect). The determination of the effective ion "damping rate" is the same as presented earlier,[10] and here only the electric field is subject to correction within the time-dependent approximation. Previously, I had advocated an effective Mach number as well as field[3,10] to remedy this problem. The analysis here indicates that the field is the more appropriate way to adjust the sheath solution for the time dependent situation.

Another new item is the use of the ambipolar theory to describe the plasma all the way to the wall boundary condition region. This has no doubt been done before, but the argument for acceptability is novel.

Page Inserted for Caption-Plot Phasing

Figure Caption

Fig.1 These are phase-space plots of velocity, field, and density *vs.* potential. The *solid* lines in these figures denote the numerical solution to Eq.(26) in the text. This particular solution has been obtained with parameter $\varepsilon = 0.01$. The starting conditions for the numerical solution are $u_o = 0.5$ and E_o given by Eq.(27) at $\phi = \phi_o = 0$. The density was simply defined as $n_i = u_o / u$. The *dotted* curves are the region IIA approximations as given in Eq.(27). The density is defined the same as in the numerical solution. The *dashed* curves are the region III approximations as given in Eq.(35). The match point occurs at $\phi = \ln(0.5) \approx -0.693$. One can see that coincidence of the dotted and solid curves for $\phi \geq -0.5$ (to the right of the match point) demonstrates that the region IIA approximations are asymptotically good. The region III approximations are valid to the left of the match point.

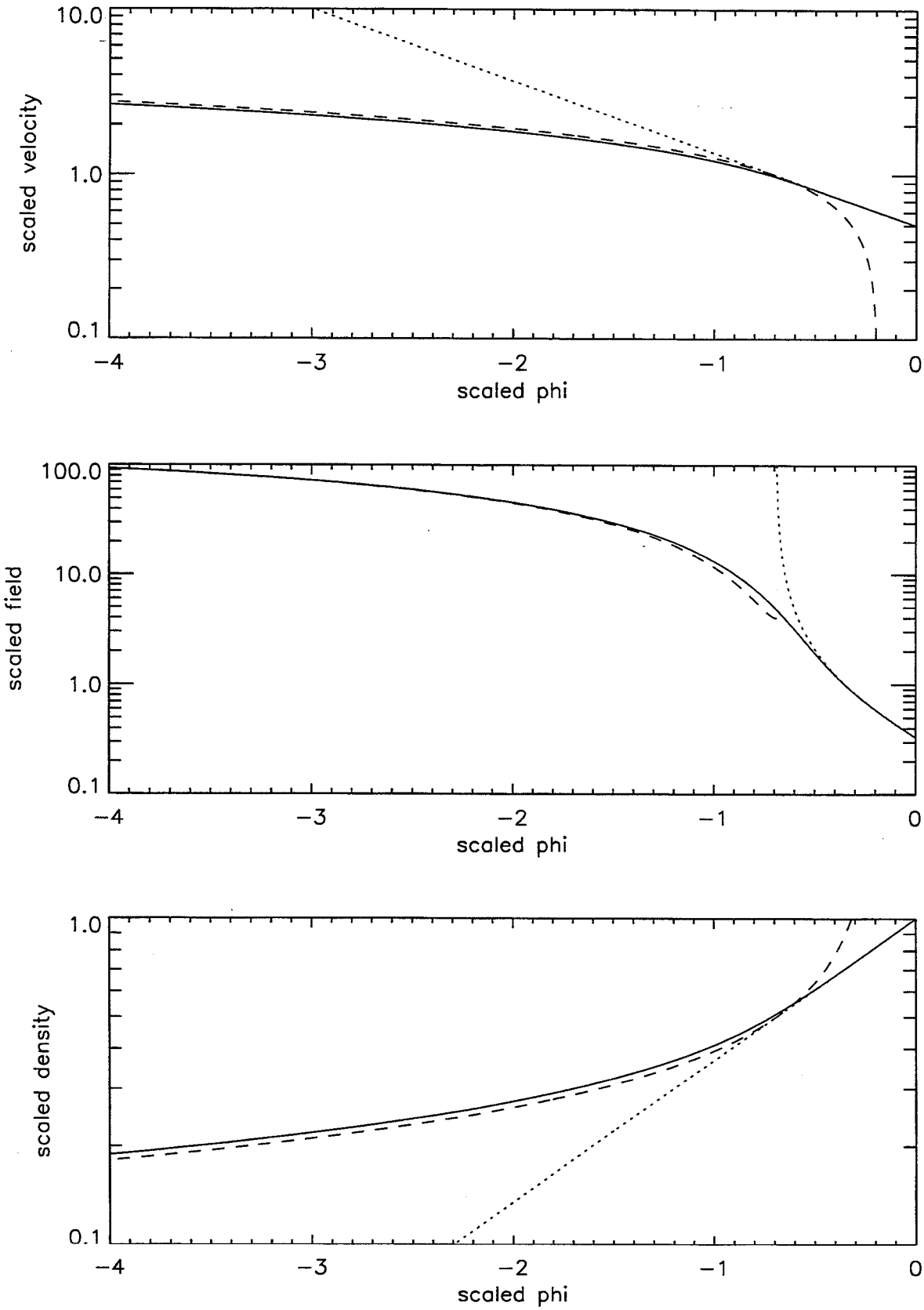
10.0
1.0
0.1
scaled velocity
−4
−3
−2
−1
0
scaled phi
100.0
10.0
1.0
0.1
scaled field
−4
−3
−2
−1
0
scaled phi
1.0
0.1
scaled density
−4
−3
−2
−1
0
scaled phi

Figure 1

Figure Caption

Fig.2 The same as Fig.1, except that only the field is being shown in all three plot panes. The upper pane is the same as given in Fig.1, the center pane has the first order displacement term removed, so that the region III approximation is that of Eq.(34), and the lower pane uses the ambipolar approximation for E, namely $E=u^2$, for the region IIA.

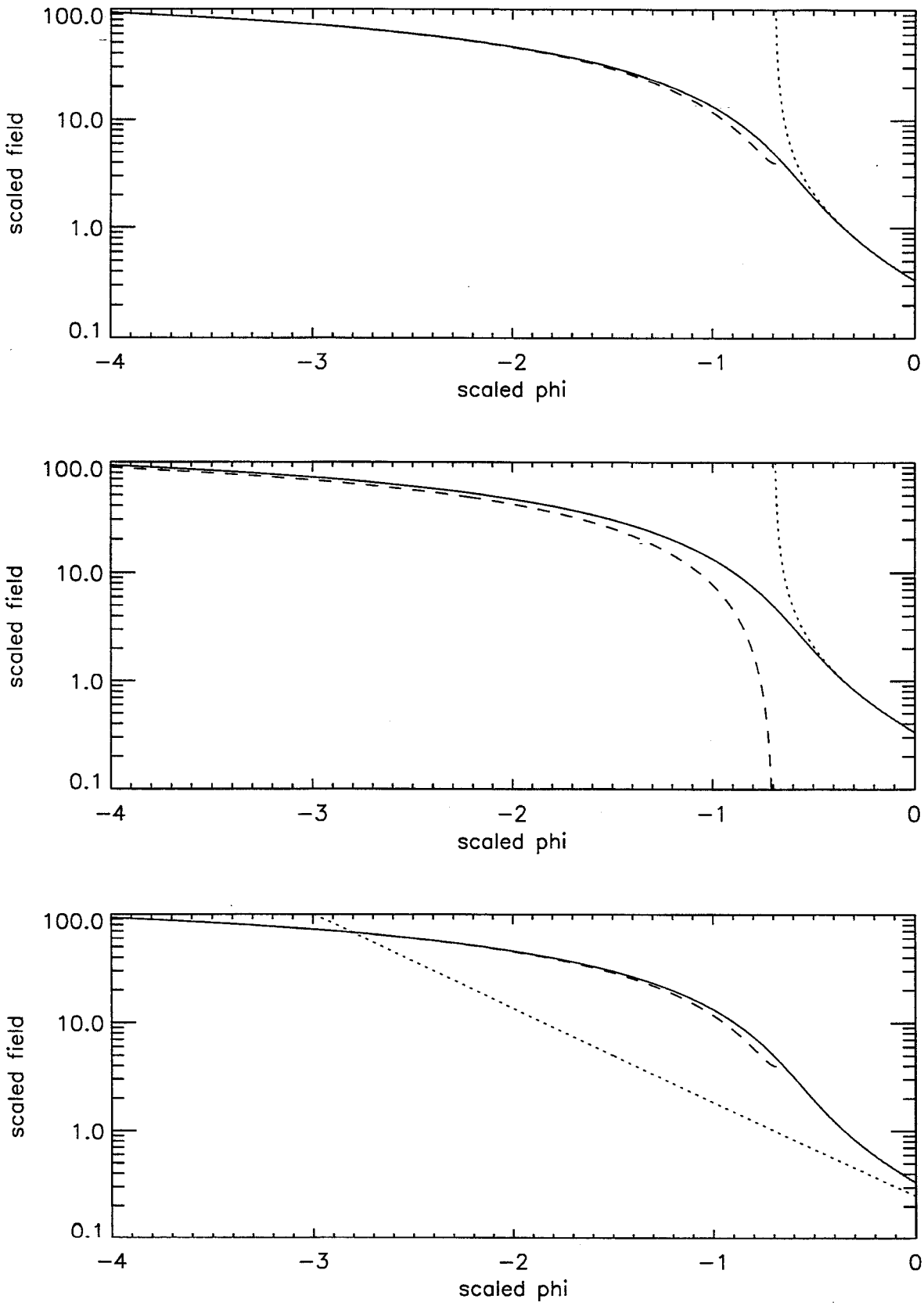
100.0
10.0
1.0
0.1
scaled field
−4
−3
−2
−1
0
scaled phi
100.0
10.0
1.0
0.1
scaled field
−4
−3
−2
−1
0
scaled phi
100.0
10.0
1.0
0.1
scaled field
−4
−3
−2
−1
0
scaled phi

Figure 2

Figure Caption

Fig.3 These are plots of the space dependences of the velocity, field, and density. The conditions are the same as in Fig.1. The left and right sides are reversed from the phase-space plot in Figs. 1 and 2. The space dependence of the approximations is found using the $s(\phi)$ mapping from the numerical solution to $ds / d\phi = -1 / E$ (field definition). Note the different perspective as to the size of the regions compared to the plots in Figs.1 and 2. It is also interesting to note that the region IIA approximation for the plasma (ion or electron) density, as given by the dotted line, becomes the region III prediction of the *electron* density on the RHS of the Bohm point at $s_1 \approx 0.83$. This may be seen from Eq.(24), which gives the exact $n_e(\phi)$ throughout regions IIA and III, and Eq.(27), which gives the *same* result from the region IIA approximation when $\phi(s)$ is inserted from the numerical integration.

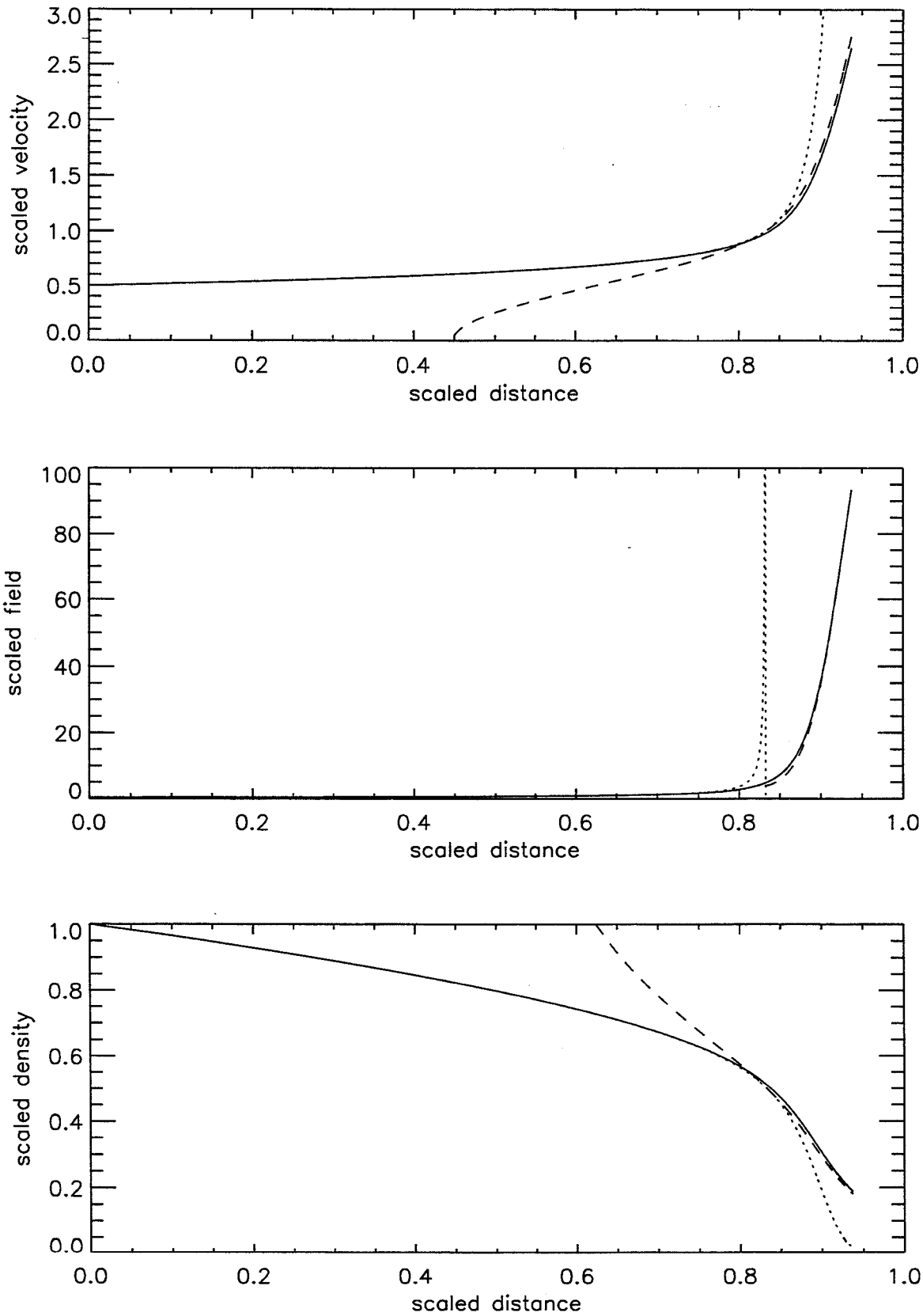
scaled velocity
3.0
2.5
2.0
1.5
1.0
0.5
0.0
0.0
0.2
0.4
0.6
0.8
1.0
scaled distance
scaled field
100
80
60
40
20
0
0.0
0.2
0.4
0.6
0.8
1.0
scaled distance
scaled density
1.0
0.8
0.6
0.4
0.2
0.0
0.0
0.2
0.4
0.6
0.8
1.0
scaled distance

Figure 3

Figure Caption

Fig.4 The same as Fig.3, except that only the field is being shown in all three plot panes and the scale is back to logarithmic to better show the comparisons. The upper pane is the same as given in Fig.3, the center pane has the first order displacement term removed, so that the region III approximation is that of Eq.(34), and the lower pane uses the ambipolar approximation for E, namely $E=u^2$, for the region IIA.

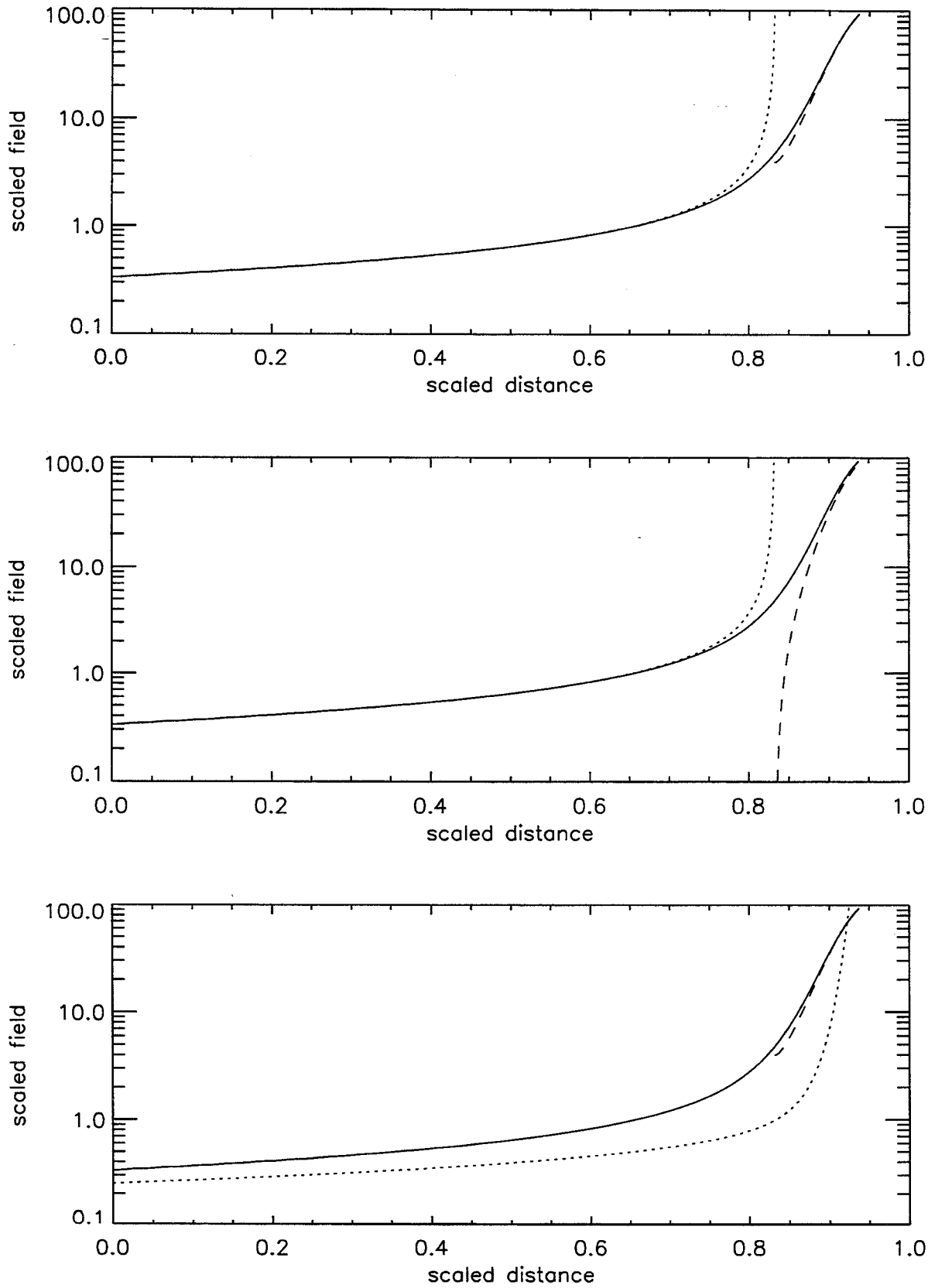
100.0
10.0
1.0
0.1
scaled field
0.0
0.2
0.4
0.6
0.8
1.0
scaled distance
100.0
10.0
1.0
0.1
scaled field
0.0
0.2
0.4
0.6
0.8
1.0
scaled distance
100.0
10.0
1.0
0.1
scaled field
0.0
0.2
0.4
0.6
0.8
1.0
scaled distance

Figure 4

Figure Caption

Fig.5 These are plots of the space dependences of the velocity, field, and density. The conditions are the same as in Fig.1 except that the mapping of the $s(\phi)$ function for the approximate solutions is obtained from the approximate $ds / d\phi = -1 / E(\phi)$ in each region. $u(s)$ is a multiple-valued function because of the structure of Eq.(21).

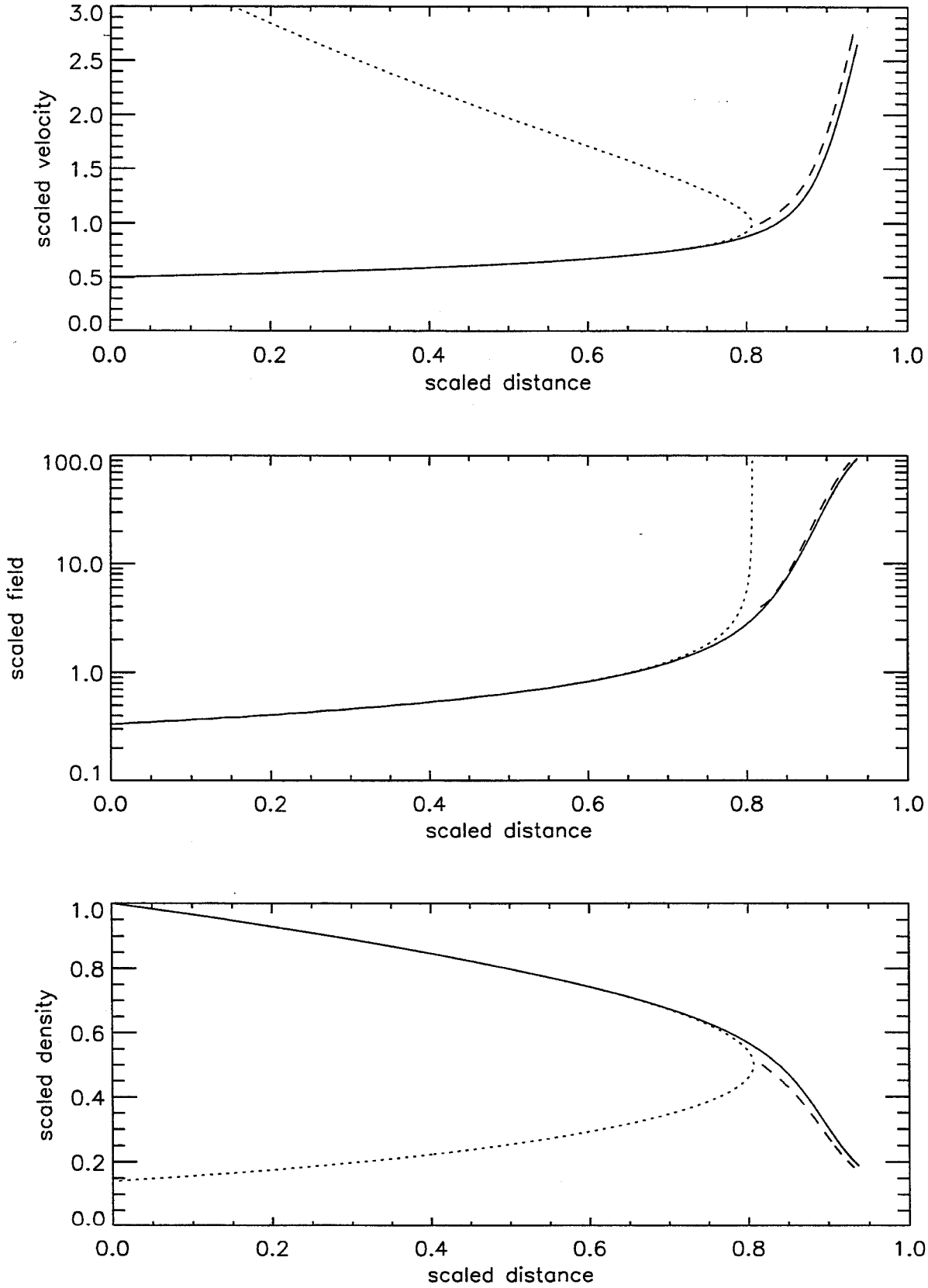
3.0
2.5
2.0
1.5
1.0
0.5
0.0
scaled velocity
0.0
0.2
0.4
0.6
0.8
1.0
scaled distance
100.0
10.0
1.0
0.1
scaled field
0.0
0.2
0.4
0.6
0.8
1.0
scaled distance
1.0
0.8
0.6
0.4
0.2
0.0
scaled density
0.0
0.2
0.4
0.6
0.8
1.0
scaled distance

Figure 5

Figure Caption

Fig.6 These are plots of the space dependences of the velocity, field, and density using the ambipolar equations for the region IIA approximation. This figure should be compared to Fig. 5, which used the quasineutral equations for IIA. The conditions are the same as in Figs.1 and 3 except that the mapping of the $s(\phi)$ function for the approximate solutions is obtained from the appropriate approximate $ds / d\phi = -1 / E(\phi)$ for each region.

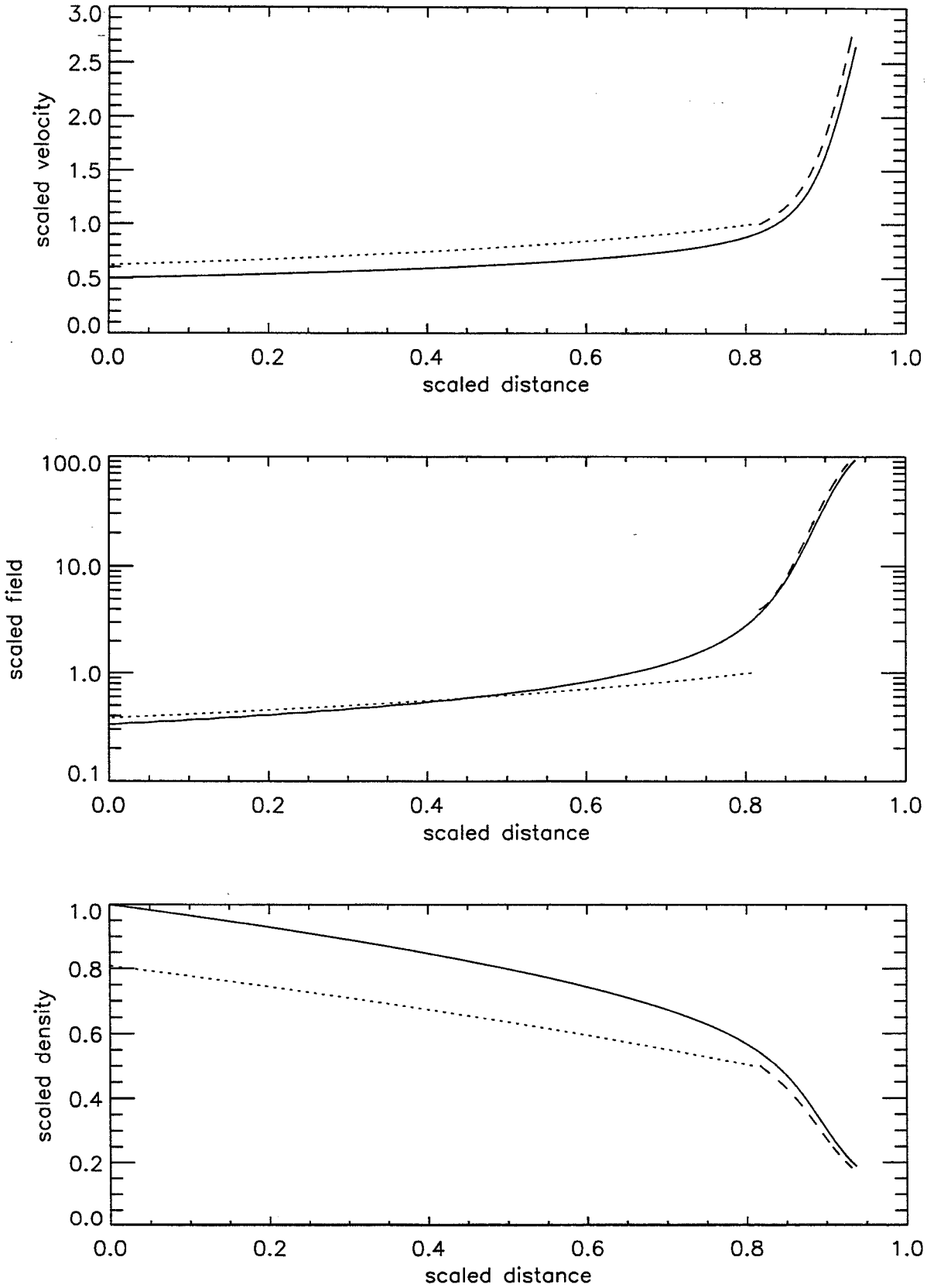
3.0
2.5
2.0
1.5
1.0
0.5
0.0
scaled velocity
0.0
0.2
0.4
0.6
0.8
1.0
scaled distance
100.0
10.0
1.0
0.1
scaled field
0.0
0.2
0.4
0.6
0.8
1.0
scaled distance
1.0
0.8
0.6
0.4
0.2
0.0
scaled density
0.0
0.2
0.4
0.6
0.8
1.0
scaled distance

Figure 6

Figure Caption

Fig.7 These are plots of the periodic time dependences of the wall values of the potentials, field, and currents. The DC current is zero and the AC is $60\,A/m^2$ as written in Eq.(60). The solid curve in the top pane is the actual potential relative to the sheath Bohm point, and the dotted curve is the effective ion potential which governs the ion impact energy. The center pane displays the wall electric field. In the lower pane, the solid curve is the total current, the dotted curve is the electron particle current, and the dashed line is the electron displacement current. The ion current is a constant ($\approx 50\,A/m^2$) as given in Eq.(59).

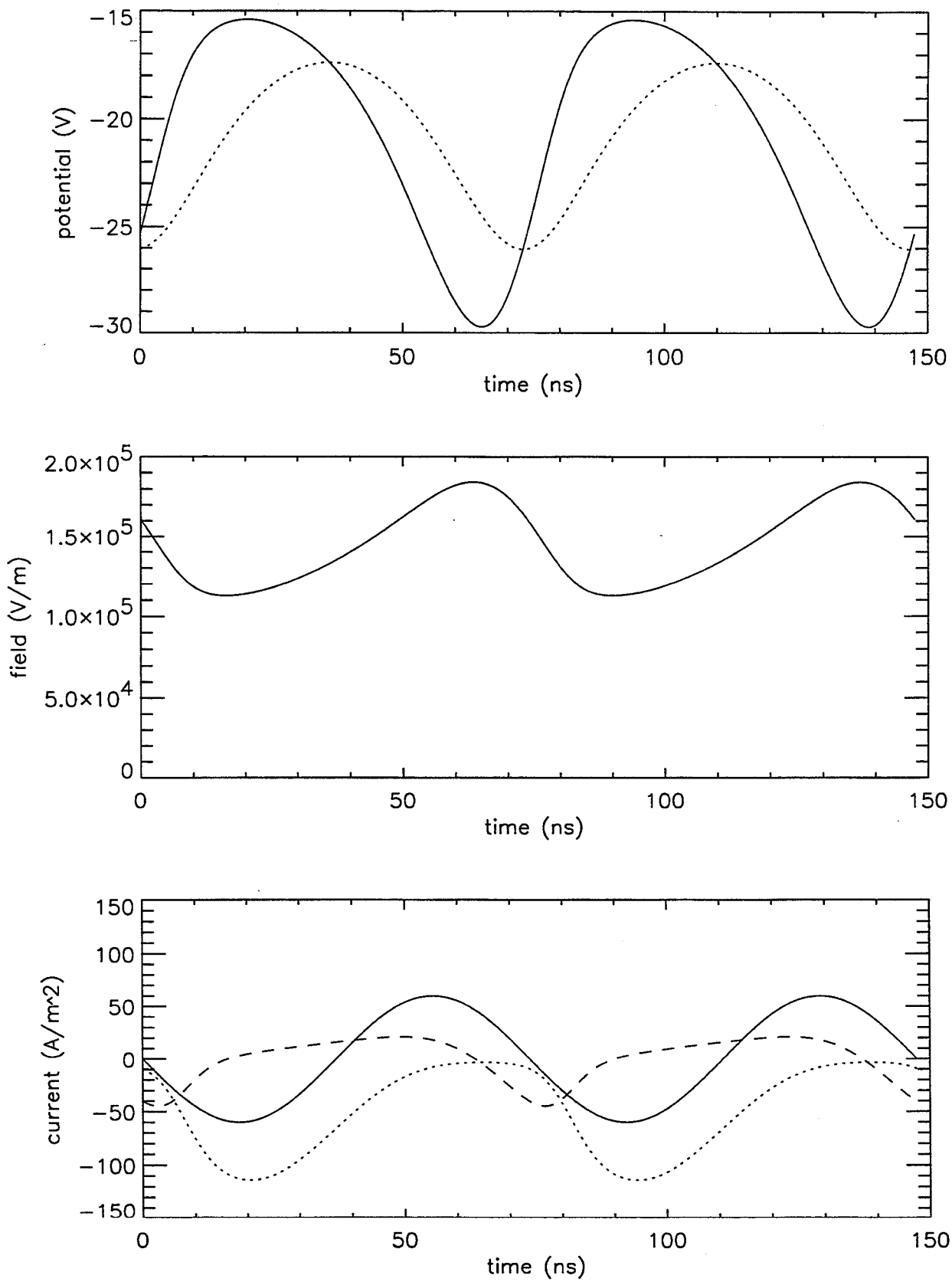
potential (V)
−15
−20
−25
−30
0
50
100
150
time (ns)
field (V/m)
2.0×10^5
1.5×10^5
1.0×10^5
5.0×10^4
0
0
50
100
150
time (ns)
current (A/m^2)
150
100
50
0
−50
−100
−150
0
50
100
150
time (ns)

Figure 7

Figure Caption

Fig.8 Same as Fig.7 except that the AC current amplitude is $160\,A/m^2$. Note the much larger variation in the wall field.

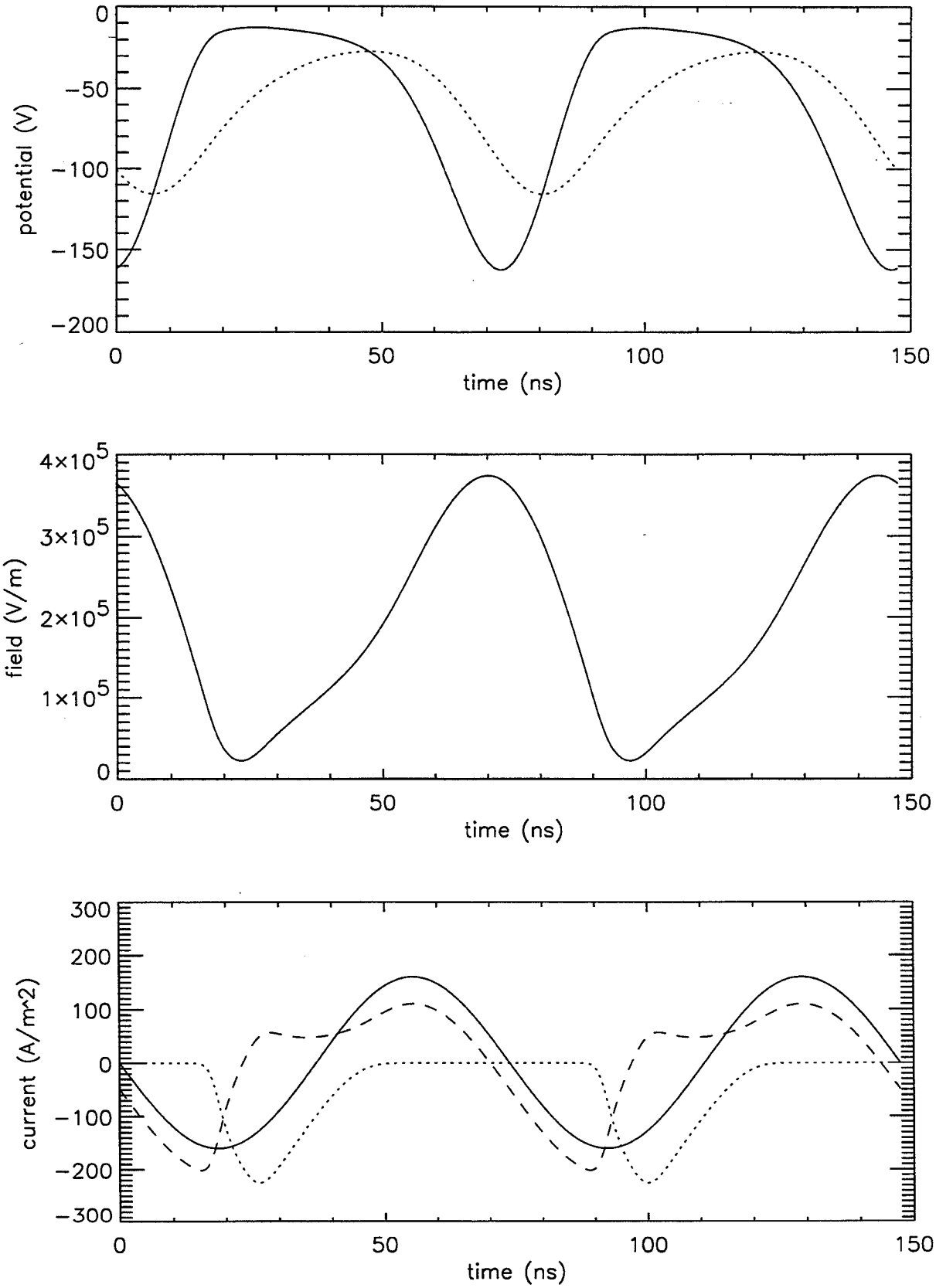
potential (V)
0
−50
−100
−150
−200
0
50
100
150
time (ns)
field (V/m)
4×10^5
3×10^5
2×10^5
1×10^5
0
0
50
100
150
time (ns)
current (A/m^2)
300
200
100
0
−100
−200
−300
0
50
100
150
time (ns)

Figure 8

Figure Caption

Fig.9 Same as Fig.7 except that the damping time constant, ω_{ip}^{-1}, has been set to 0.1ns to force the effective ion potential to follow the actual potential just as in the the QSS (Metze, Ernie, and Oskam) model. In the top pane the potentials coincide to graphical accuracy. For these lower current conditions, the QSS is quite good.

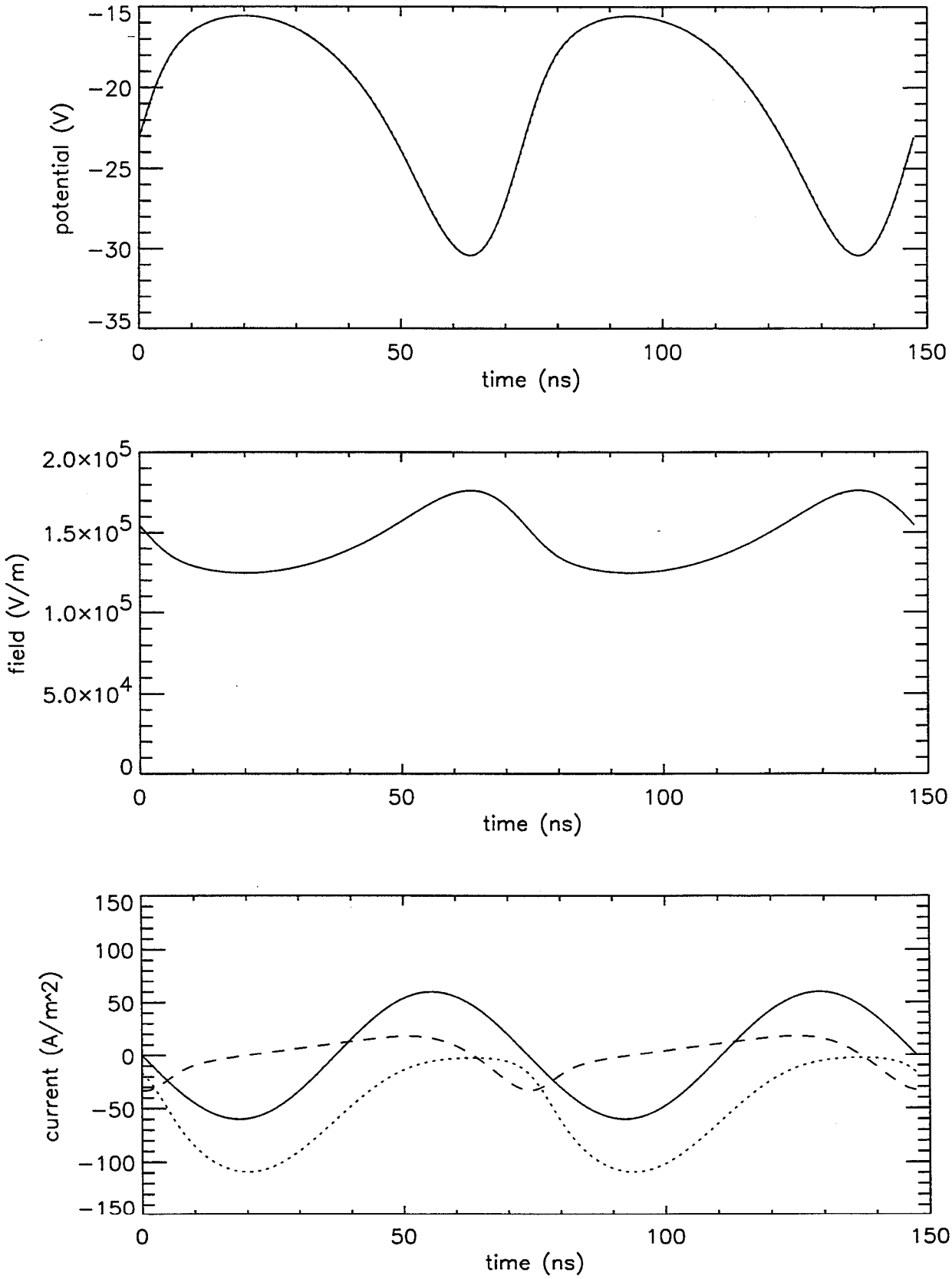
potential (V)
−15
−20
−25
−30
−35
0
50
100
150
time (ns)
field (V/m)
2.0×10^5
1.5×10^5
1.0×10^5
5.0×10^4
0
0
50
100
150
time (ns)
current (A/m^2)
150
100
50
0
−50
−100
−150
0
50
100
150
time (ns)

Figure 9

Figure Caption

Fig.10 Same as Fig.8 except that the damping time constant, ω_{ip}^{-1}, has been set to 0.1ns to force the effective ion potential to follow the actual potential just as in the the QSS (Metze, Ernie, and Oskam) model. In the top pane the potentials coincide to graphical accuracy. The QSS is not very accurate for this higher current case.

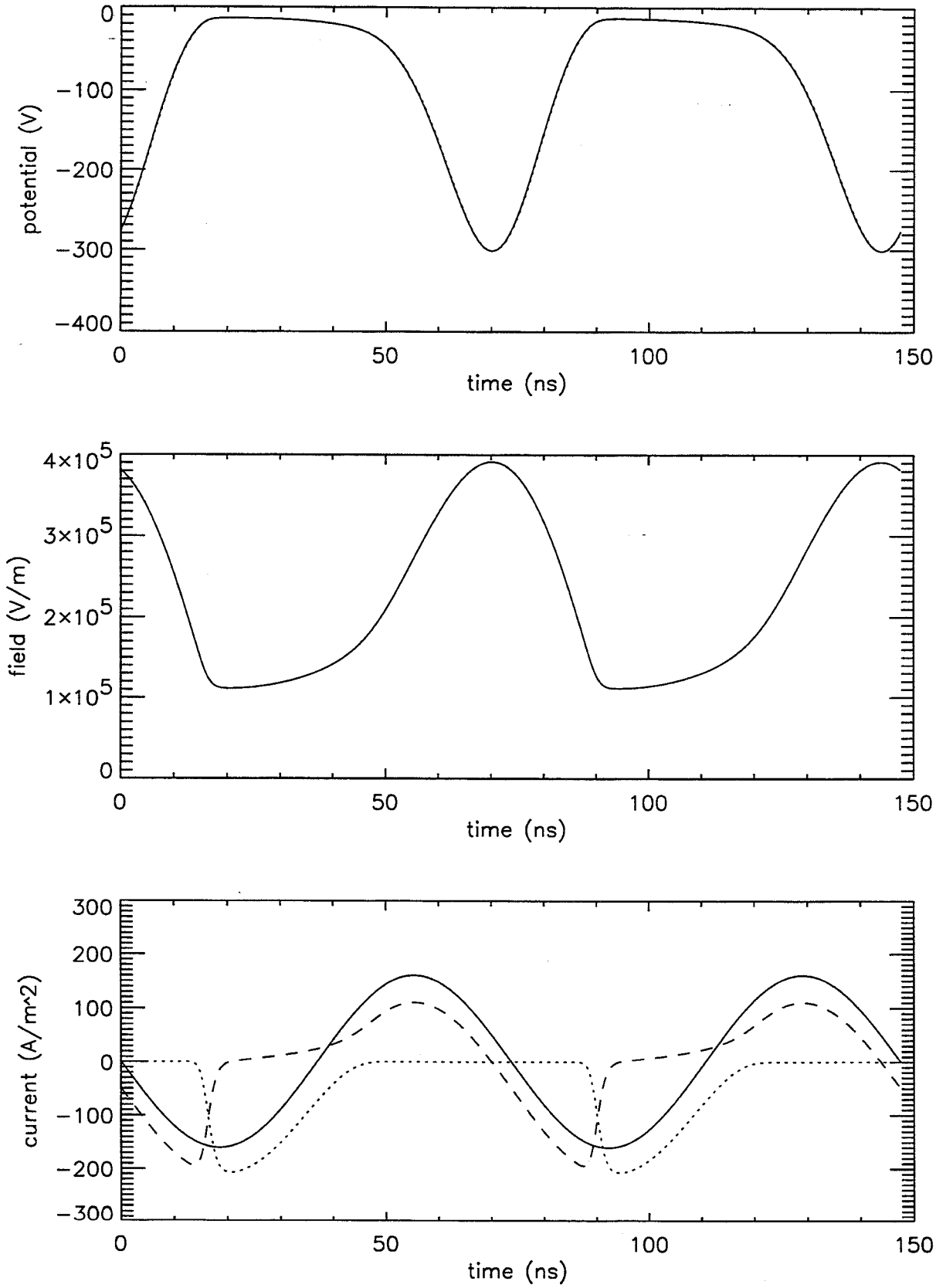
0
−100
−200
−300
−400
potential (V)
0
50
100
150
time (ns)
4×10^5
3×10^5
2×10^5
1×10^5
0
field (V/m)
0
50
100
150
time (ns)
300
200
100
0
−100
−200
−300
current (A/m^2)
0
50
100
150
time (ns)

Figure 10

Figure Caption

Fig.11 The numerical solutions for the potentials, field, and currents for the sheath model with the AC current amplitude set at $j_{ac} = 200\,A/m^2$. For this current, the integration constant $E_0(t)$ is allowed to float up and down as necessary in order to keep the root of Eq.(52) real. $E_0(t)$ is nonzero only in the flat spots seen in the field plot in the center pane at the minima of the curve. The parameters of the plasma are given in Eqs.(58) and (59).

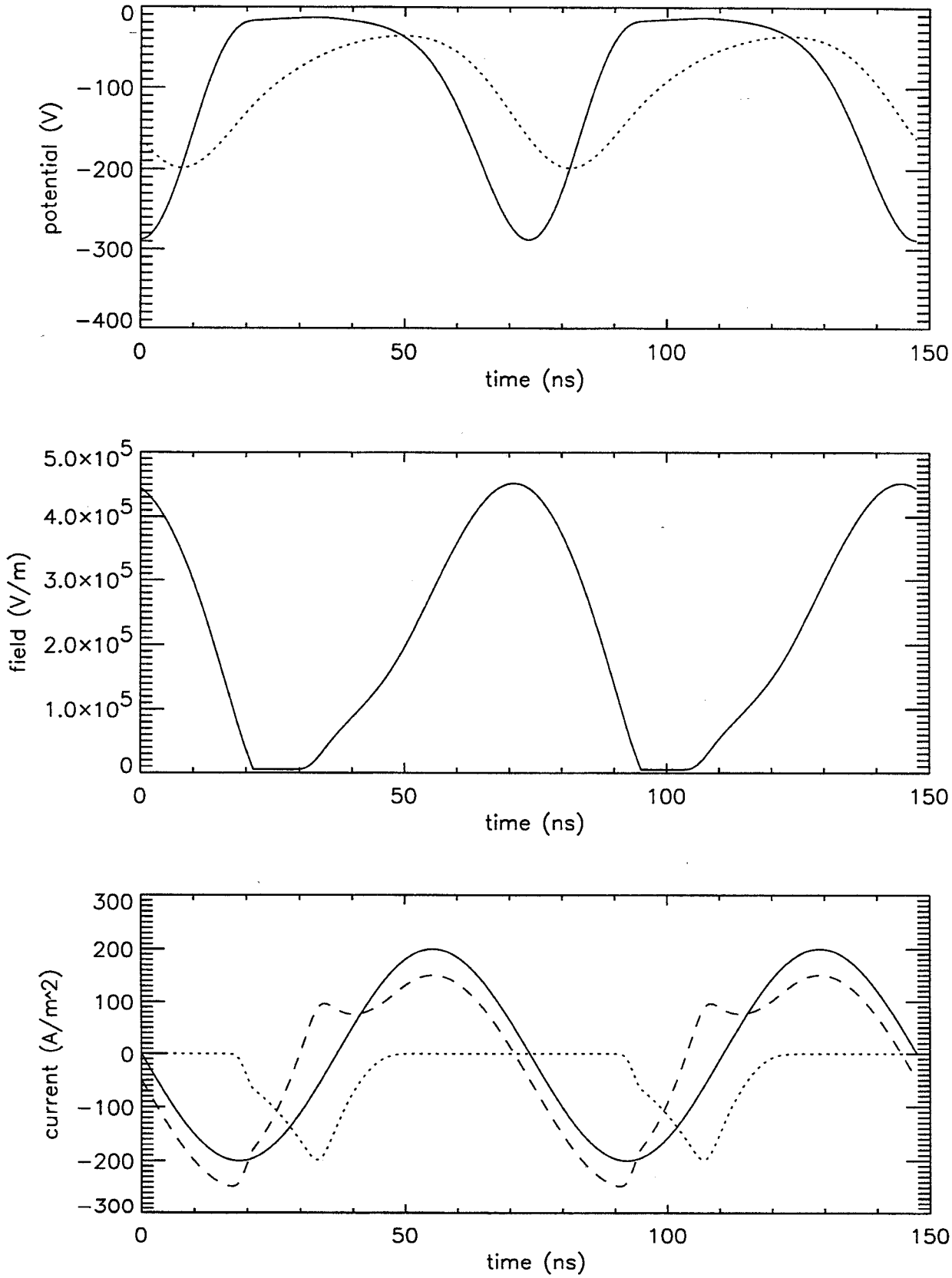
0
−100
−200
−300
−400
potential (V)
0
50
100
150
time (ns)
5.0×10^5
4.0×10^5
3.0×10^5
2.0×10^5
1.0×10^5
0
field (V/m)
0
50
100
150
time (ns)
300
200
100
0
−100
−200
−300
current (A/m^2)
0
50
100
150
time (ns)

Figure 11

Figure Caption

Fig.12 Same as Fig.11 except that the integration constant $E_0(t)$ is allowed to rise to a constant value such that the root does not become imaginary. The value found from the integration was 51.6 kV/m (516 V/cm) which is a small value compared to the peak wall field of roughly 450 kV/m. However it is large compared to the E_1 value of 5 kV/m. Recall that E_1 is the QSS value of the field at the Bohm point in the bulk-to-sheath transition region III.

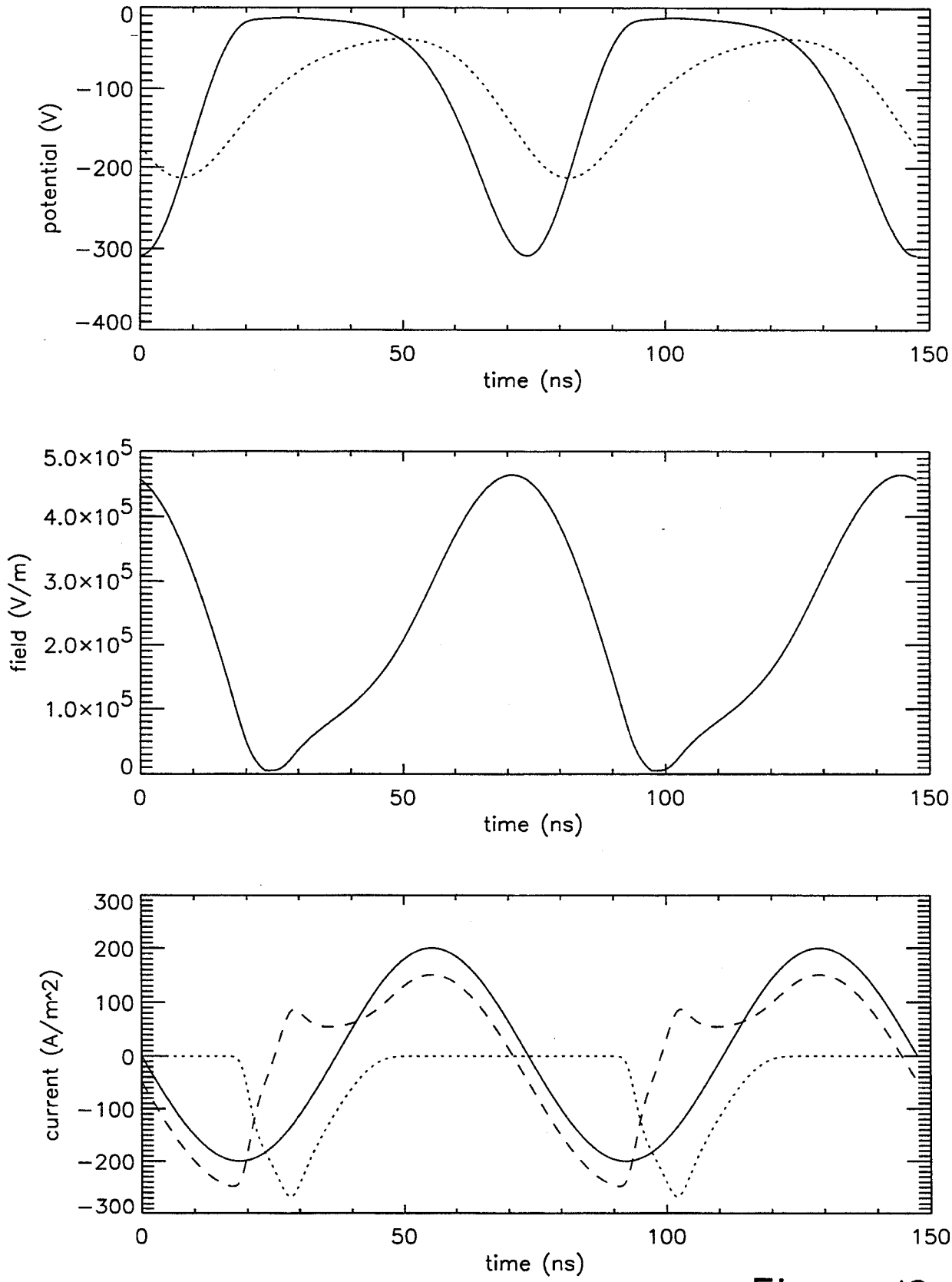
potential (V)
0
−100
−200
−300
−400
0
50
100
150
time (ns)
field (V/m)
5.0×10^5
4.0×10^5
3.0×10^5
2.0×10^5
1.0×10^5
0
0
50
100
150
time (ns)
current (A/m^2)
300
200
100
0
−100
−200
−300
0
50
100
150
time (ns)

Figure 12

References

1. M. A. Lieberman, "Analytical Solution for Capacitive RF Sheath," IEEE Transactions on Plasma Science, **16**, 638-644 (1988).

2. A. Metze, D. W. Ernie, and H. J. Oskam, "Application of the physics of plasma sheaths to the modeling of rf plasma reactors," J. Appl. Phys. **60**, 3081-3087 (1986).

3. Merle E. Riley, "Unified Model of the rf Plasma Sheath," Sandia National Laboratories Technical Report SAND95-0775 UC-401, printed May 1995.

4. F. F. Chen, "Introduction to Plasma Physics and Controlled Fusion," Vol. 1, Plenum, NY, NY, p290-ff. (1988).

5. David Bohm, "The Characteristics of Electrical Discharges in Magnetic Fields," eds. A. Guthrie and R.K. Wakerling, McGraw Hill, NY, NY, Ch. 3 (1949).

6. Valery A. Godyak and Natalia Sternberg, "Smooth Plasma-Sheath Transition in a Hydrodynamic Model," IEEE Trans. on Plasma Sci., **18**, 159-168 (1990).

7. Peter C. Stangeby, "The Plasma Sheath," in "Physics of Plasma-Wall Interactions in Controlled Fusion," D.E. Post and R. Behrisch, eds.,Plenum, NY, NY, pp 41-97 (1986).

8. Wolfgang Wasow, "Asymptotic Expansions for Ordinary Differential Equations," Ch. 10, Interscience, NY, NY, (1965).

9. V. A. Godyak, "Modified Bohm Criterion for a Collisional Plasma," Phys. Lett. **89A**, 80-81 (1982).

10. M. E. Riley, "Unified Model of the rf Plasma Sheath," Talk QA5, 48th Annual Gaseous Electronics Conference, Oct. 9-13, 1995, Berkeley, Calif. Published in Bull. Am. Phys. Soc. **40**, No. 9, p.1587 (1995).

11. A. M. Pointu, "Dynamics of a rf sheath in the range between the ionic and the electronic plasma frequencies," Appl. Phys. Letts. **50**, 316-317 (1986).

DISTRIBUTION:

2 Lee A. Berry
Fusion Energy Division
Oak Ridge National Lab
PO Box 2009
Oak Ridge, TN 37831

2 Professor Demetre J. Economou
Department of Chemical Engineering
University of Houston
Houston, TX 77204-4792

1 Valery A. Godyak
GTE Laboratories, Inc.
40 Sylvan Road
Waltham, MA 02254

2 Professor David Graves
Department of Chemical Engineering
University of California
201 Gilman Hall
Berkeley, CA 94720

2 Professor Mark Kushner
Electrical and Computer Engineering
University of Illinois
Urbana, IL 61801

1 Professor M. A. Lieberman
Department of Electrical Engineering
University of California
Berkeley, CA 94720

1 Peter Loewenhardt
New Product Development
Applied Materials, Inc.
Santa Clara, CA 95054

1 Sadasivan Shankar
Technology CAD Department
Intel Corporation
RN2-40 P.O. Box 58119
2200 Mission College Blvd.
Santa Clara, CA 95052-8119

1 Professor Natalia Sternberg
Department of Mathematics and Computer Science
Clark University
Worcester, MA 01610

1 Vahid Vahedi
Lam Research Corporation
4650 Cushing Parkway
Fremont, CA 94538

1 MS 1423 Paul A. Miller, 1128

1 MS 9042 Ellen Meeks, 8345

1 MS 9042 Jong Won Shon, 8345

1 MS 0827 Robert B. Campbell, 9114

1 MS 1423 Ramana Veerasingam, 9114

1 MS 0827 Timothy J. Bartel, 9114

1 MS 0827 Justine E. Johannes, 9114

10	MS 1423	Merle Riley, 1128
1	MS 9018	Central Technical Files, 8523-2
5	MS 0899	Technical Library, 4414
2	MS 0619	Review & Approval Desk, 12630 [For DOE/OSTI]